Available online at www.sciencedirect.com
ScienceDirect
Lithos 102 (2008) 478–507
LITHOS
www.elsevier.com/locate/lithos

# Age and emplacement of late-Variscan granites of the western Bohemian Massif with main focus on the Hauzenberg granitoids (European Variscides, Germany)

T. Klein [a,*], S. Kiehm [b], W. Siebel [c], C.K. Shang [c], J. Rohrmüller [d], W. Dörr [a], G. Zulauf [a]

[a] *Institut für Geowissenschaften, Altenhöferallee 1, 60438 Frankfurt am Main, Germany*
[b] *Dresdener Str. 6, 63454 Hanau, Germany*
[c] *Institut für Geowissenschaften, Universität Tübingen, Wilhelmstraße 56, 72074 Tübingen, Germany*
[d] *Bayerisches Geologisches Landesamt, Leopoldstraße 30, 95632 Marktredwitz, Germany*

Received 15 November 2006; accepted 25 July 2007
Available online 30 August 2007

**Abstract**

The Variscan Hauzenberg pluton consists of granite and granodiorite that intruded late- to postkinematically into HT-metamorphic rocks of the Moldanubian unit at the southwestern margin of the Bohemian Massif (Passauer Wald). U–Pb dating of zircon single-grains and monazite fractions, separated from medium- to coarse-grained biotite-muscovite granite (Hauzenberg granite II), yielded concordant ages of 320±3 and 329±7 Ma, interpreted as emplacement age. Zircons extracted from the younger Hauzenberg granodiorite yielded a $^{207}Pb$–$^{206}Pb$ mean age of 318.6±4.1 Ma. The Hauzenberg granite I has not been dated. The pressure during solidification of the Hauzenberg granite II was estimated at 4.6±0.6 kbar using phengite barometry on magmatic muscovite, corresponding to an emplacement depth of 16-18 km. The new data are compatible with pre-existing cooling ages of biotite and muscovite which indicate the Hauzenberg pluton to have cooled below $T$=250–400 °C in Upper Carboniferous times. A compilation of age data from magmatic and metamorphic rocks of the western margin of the Bohemian Massif suggests a west- to northwestward shift of magmatism and HT/LP metamorphism with time. Both processes started at >325 Ma within the South Bohemian Pluton and magmatism ceased at ca. 310 Ma in the Bavarian Oberpfalz. The slight different timing of HT metamorphism in northern Austria and the Bavarian Forest is interpreted as being the result of partial delamination of mantle lithosphere or removal of the thermal boundary layer.


*Keywords:* Bohemian Massif; Hauzenberg granite; U–Pb geochronology; Phengite barometry; Variscides

## 1. Introduction

The internal part of the Variscan belt (termed 'Moldanubian unit' by Kossmat, 1927) is characterized by a Carboniferous high-heat flow event. This is documented by more or less penetrative high-temperature metamorphism and related anatexis, followed by the emplacement of numerous granitoid plutons. In the

* Corresponding author.
*E-mail addresses:* T.Klein@em.uni-frankfurt.de (T. Klein), skiehm@web.de (S. Kiehm), wolfgang.siebel@uni-tuebingen.de (W. Siebel), cosmas@uni-tuebingen.de (C.K. Shang), Johann.Rohrmueller@gla.bayern.de (J. Rohrmüller), wolfgang.doerr@geolo.uni-giessen.de (W. Dörr), g.zulauf@em.uni-frankfurt.de (G. Zulauf).

0024-4937/$ - see front matter © 2007 Elsevier B.V. All rights reserved.
doi:10.1016/j.lithos.2007.07.025

Bohemian Massif this event has been dated at 340–320 Ma (U–Pb dating on zircon (Van Breemen et al., 1982) and monazite (Van Breemen et al., 1982; Teufel, 1988; Friedl et al., 1993, 1994; Kalt et al., 2000). During anatexis an incredible amount of melt was generated. Assuming a spherical shape for all Carboniferous plutonic rocks in the Moldanubian Zone of the Bohemian Massif, Behrmann and Tanner (1997) calculated a minimum volume of 176,000 $km^3$ of magmatic crust, which amounts to approximately 25% of the overall crustal volume in this area. This estimate is reasonable since gravimetric investigations of the subsurface distribution of granites from the northern Oberpfalz revealed basal depths of 3–8 km, which is in most cases slightly less than the radius of the specific plutons (Trzebski et al., 1997; their Table 2). Within the South Bohemian Pluton, above average radiogenic heat production of ca. 5.0 $\mu Wm^{-2}$ and normal heat flux point to basal depths below ca. 6 km (Vellmer and Wedepohl, 1994).

Granitoids are either older or younger than the phase of high heat flow (Klečka and Matějka, 1992; Finger et al., 1997; Holub et al., 1997; Siebel et al., 1997). However, a relation between HT-metamorphism and the occurrence of post-collisional S-type granites seems to exist, particularly in the Bavarian Forest.

Most of the Variscan granites within the Moldanubian unit intruded postkinematically. Examples of synkinematic granitoids are the granodioritic intrusions at the Bavarian Lode shear zone (so-called Palites) or the fine-grained Lásenice granite at the NW contact of the main body of the South Bohemian Pluton. The latter is affected by a shear-zone that cannot be recognized within the main facies of the pluton. Similarly, the Lipnice granite in the N part of the pluton is affected by flat extensional shearing, which is missing in younger intrusions. The magma of the muscovite-bearing Lásenice granite probably formed by minimum melting during the thermal peak of regional metamorphism (Breiter and Koller, 1999). Synkinematic plutons also straddle the Bohemian Shear Zone at the Moldanubian/Tepla-Barrandian boundary (Fig. 1; Siebel et al., 1999; Scheuvens and Zulauf, 2000; Zulauf et al., 2002).

The processes which led to high heat flow and crustal melting are not fully understood yet. A recent discussion of different conceptual models that might explain high heat flow and related late- to postcollisional magmatism within the Variscides can be found in Henk et al. (2000). A general geochemical and geochronological classification of European Variscan plutonic rocks is given in Finger et al. (1997).

The Hauzenberg pluton consists of three individual late- to postkinematic felsic intrusions within the Moldanubian part of the southwestern Bohemian Massif (Fig. 1). As other granites of the southeastern Bavarian Forest the Hauzenberg pluton might represent the westernmost part of the South Bohemian Pluton.

New U–Pb ages of zircon single-grains and monazite fractions separated from the Hauzenberg granite II, mean Pb–Pb zircon-evaporation ages obtained with the Kober-method (Kober, 1986) for the Hauzenberg granodiorite, which crosscuts the older granites, as well as geobarometric data for the Hauzenberg granite II and for a sheared granite dyke, located about 1 km south of the main pluton (Taxberg), are presented.

These data are discussed together with published geochronological data of metamorphic and granitoid rocks: as many age data reported from the Bohemian massif are not accessible through international journals, we decided to include a compilation of ages reported from the Moldanubian unit in Germany and Austria (see Section 5). We greatly benefited from prior compilations (Teufel, 1988; Finger et al., 1997; Siebel, 1998; Propach et al., 2000; Siebel et al., 2003). The focus of the compilation lies on magmatic U–Pb ages which have been interpreted as emplacement ages. K–Ar mica, $^{207}Pb$–$^{206}Pb$ zircon and Rb–Sr whole-rock and mineral age data are included as well. The corresponding publications also might contain other geochemical and/or petrographical information of interest. The reader should be aware of discrepancies between U–Pb mineral ages and Rb–Sr whole rock isochrons. A possible danger is the misinterpretation of an obtained U–Pb zircon or monazite age in case of unrecognised inheritance, whereas Rb–Sr whole rock isochrons often are meaningless, due to the polyphase metamorphism, anatexis of Moldanubian rocks and magma mixing. Additionally, their resolution is in many cases poor. On the other hand Rb–Sr mineral ages should yield relatively reliable cooling ages, since extensive post-Variscan heating is lacking. In some cases the Rb–Sr system has been reset by fluid activity (Siebel et al., 2005b).

Although the concept of isotopic closure of distinct isotope/mineral pairs is debatable (Villa, 1998), consideration of concordant U–Pb and $^{207}Pb$–$^{206}Pb$ ages with minor spreads of zircon and monazite as intrusion ages appears valid (c.f. Lee et al., 1997; Mezger and Krogstad, 1997; Cherniak and Watson, 2001, 2004), particularly if they rely upon measurements of single-grains. The few U–Pb ages of titanite are considered as crystallization ages. Isotopic closure of titanite occurs at temperatures much lower than those of the aforementioned minerals, approximately close to the granitic solidus (e.g. Cherniak, 1993; Scott and St-Onge, 1995).

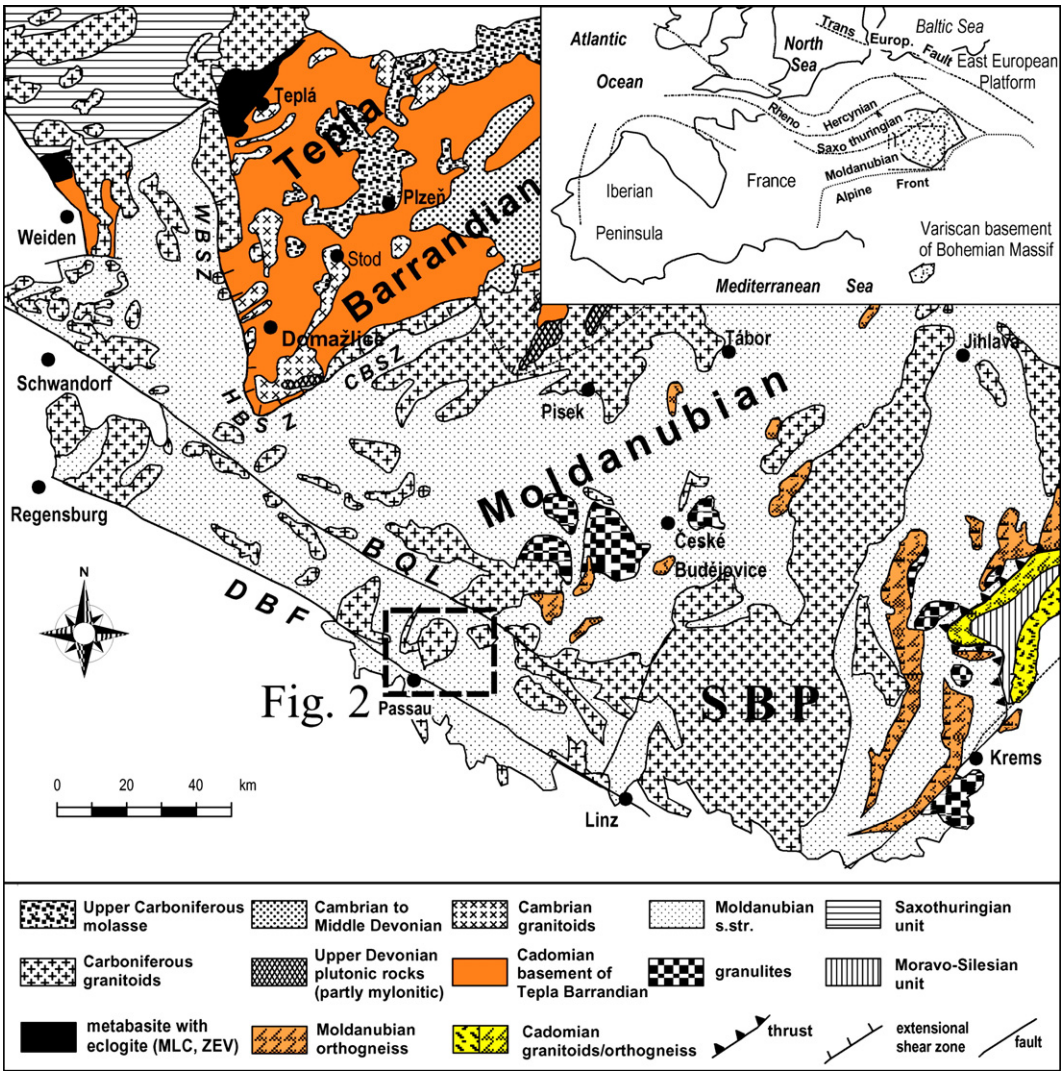


Fig. 1. Geological sketch map of the Bohemian Massif: DBF = Danubian fault, BQL = Bavarian Lode shear zone, WBSZ = West Bohemian shear zone, HBSZ = Hoher Bogen shear zone, CBSZ = Central Bohemian shear zone, SBP = South Bohemian pluton. Box indicates the area shown in detail map of the Hauzenberg pluton (Fig. 2).

Thus, for the given regional setting, thermal resetting of titanites is likely for grains older than ca. 320 Ma. The remaining systems, specifically K–Ar and Rb–Sr ages of muscovite and biotite are indicative for substantial cooling below solidus temperatures of granitoids ($T$ < 500 °C). Particularly these isotopic ages might be affected by later fluid related processes that occurred at greenschist facies conditions. However, strong retrogression is bound to fault zones and easily recognized by the neoformation of minerals such as epidote, clinozoisite, actinolite and chlorite.

New and existing data are combined to draw a model that interprets 1) magmatism to result from slight but significant decompression and 2) the initial cause of Variscan high heat flow to be (partial) delamination of the lithospheric mantle.

## 2. Regional geology

The investigated rocks are located in the southern Bavarian Forest (Passauer Wald) between the Danubian fault (Donau–Störung) and the Bavarian Lode shear zone (Bayerischer Quarzpfahl). The latter was formed within a NW-SE trending dextral strike-slip shear zone (Fig. 1) along which granitoid melts and large amounts of fluids migrated (Troll, 1967b; Siebel et al., 2005a), the latter causing extensive precipitation of quartz.

In map view the Hauzenberg pluton has an elliptical shape with long and short axes of 11 and 8 km, respectively (Fig. 2). It consists of three distinct intrusions (Fig. 2; for further details, see Dollinger, 1967) that are enumerated with roman numbers, which reflect the sequence of their emplacement:

*Hauzenberg granite I* (ca. 20% of the pluton area), characterized by fine- to medium-grained biotite–muscovite granite with enclaves rich in biotite and muscovite. These enclaves might result from breakdown of cordierite or andalusite/sillimanite. Accessory minerals are zircon, apatite, garnet, and opaque phases. K–Ar dating yielded 284±3 and 313±3 Ma for muscovite and 293±3 Ma for biotite. Rb–Sr dating of biotite yielded 310±3 Ma (all data from Harre et al., 1967).

*Hauzenberg granite II* (ca. 50% of the pluton area), consisting of medium- to coarse-grained biotite-muscovite granite, which has a similar geochemical composition as the Hauzenberg granite I. Accessory minerals include zircon, apatite, andalusite, sillimanite

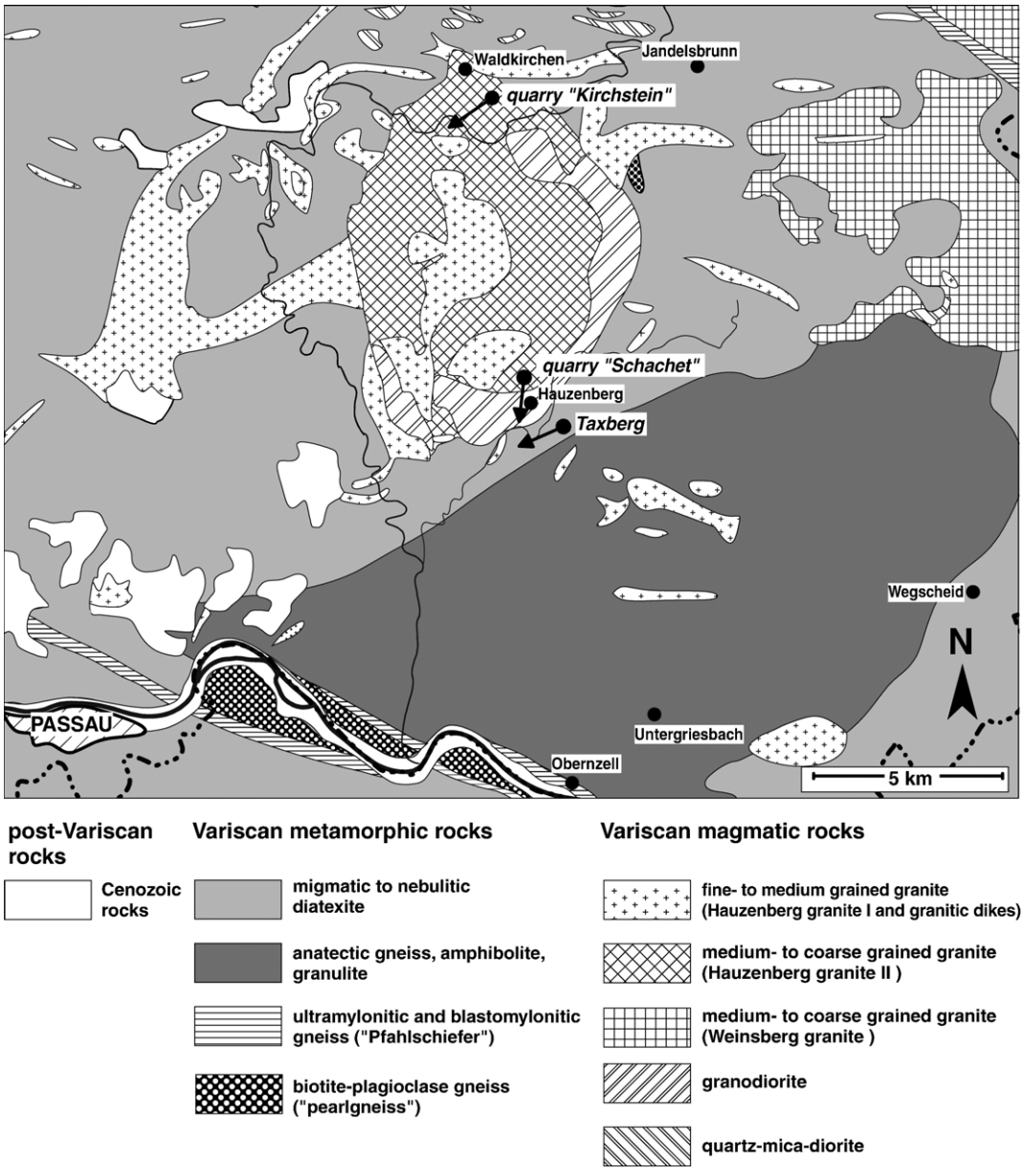


Fig. 2. Geological map of the Hauzenberg granite (modified after Troll, 1967b) and sample localities.

and cordierite. Isotopic analyses yielded a minimum age for the emplacement of the Hauzenberg granite II of 312±6 Ma (Rb–Sr mineral isochron) and an initial ratio of $^{87}Sr/^{86}Sr$ at 0.7089 (Christinas et al., 1991b). Zr-saturation points to initial melt temperatures of ca. 780 °C (method of Watson and Harrison, 1983 based on X-ray fluorescence analyses; own and supplementary data by Olbrich, 1985).

*Hauzenberg granodiorite*, fine- to medium-grained, juxtaposed against the above granites in the eastern and southern part of the massif. Primary minerals are biotite, plagioclase, K-feldspar, quartz. Accessory minerals are zircon, xenotime, monazite, apatite, magnetite, and pyrite. K–Ar dating of biotite yielded 284±4 and 294±5 Ma; Rb–Sr dating of biotite yielded 302±13 Ma (Harre et al., 1967).

The granitoids are crosscut by pegmatites, aplites, and porphyritic dykes. A porphyritic dyke (Kirchstein quarry) of granodioritic composition yielded 302±7 Ma (Rb–Sr mineral isochron) and an initial ratio of $^{87}Sr/^{86}Sr$ at 0.7059 (Christinas et al., 1991b). Although the porphyritic dykes intruded as parallel swarms, their composition is highly variable, ranging from andesitic to dacitic, locally even rhyolithic (Propach et al., in press).

The southern country rocks of the Hauzenberg pluton are anatectic gneisses with intercalations of migmatic amphibolites, calc-silicate rocks and granulites, all of which are interpreted to belong to the Variegated Group (Kropfmühl Series) of the Moldanubian unit. To the north the country rocks are anatectic paragneisses (sedimentary precursors have been constrained by Troll and Winter, 1969) that belong to the Moldanubian Monotonous Series. Ca. 10 km to the north "palites" (as defined by Frentzel, 1911) occur. These are very early synkinematic granitoids (Siebel et al., 2005a and references therein), which occur along the Bavarian Quartz Lode. The quartz mineralization, which determines the relief today, is known to have formed in early Triassic times (Horn et al., 1986).

Age relations of the individual intrusions of the Hauzenberg pluton were drawn by field observations. The oldest intrusive rocks are dykes of (grano)dioritic composition ("quartz-mica diorites"). The latter occur mainly north and northwest of the pluton where they form the "northern diorite zone" of Cloos (1927). The Hauzenberg granite I forms the roof of the pluton. It appears in the center of the massif. The contact towards the Hauzenberg granite II is often horizontal (Cloos, 1927). In cases where relative age constraints can be drawn, fine-grained granites are slightly older (Cloos, 1927; Olbrich, 1985 and references therein). Since fine-grained granite occurs as xenoliths, enclaves, dykes and even schlieren (Dollinger, 1967) within coarser grained granite, the coarser Hauzenberg granite II represents the main magmatic activity. Detailed mapping by Dollinger (1961) revealed the granodiorite to be younger than the granites.

## 3. Methods and sample localities

A 45 kg sample of the Hauzenberg granite II was collected from the Kirchstein quarry (ca. 2 km S of Waldkirchen) (Fig. 2) and preparated after Dörr et al. (2002). Heavy minerals were enriched using a Wilfley table, hand magnet and heavy liquids. Zircons have been air-abraded for 17 h following the technique of Krogh (1982). Zircons and monazites were selected microscopically according to their size and quality (absence of fractures, well-developed crystal-faces, euhedral shape) and weighted afterwards. Representative zircons were embedded in epoxy resin and polished for cathodoluminescense (CL) and backscatter electron imaging (BSI) by electron microprobe, carried out at Frankfurt University (Jeol Superprobe JXA 8900). CL images of zircons from the Hauzenberg granodiorite were made using a Zeiss DSM 960A at Munich University (LMU).

The chemical decomposition of zircon and monazite, the separation of U and Pb, and the mass spectrometric isotope analyses were performed at Giessen University using the standard procedures described by Krogh (1973) and Parrish (1987) (instrument: Finnigan MAT 261).

The used spike (Russland II) has a $^{206}Pb/^{204}Pb$ ratio of 120, $^{206}Pb/^{205}Pb$ of 0.05 and a $^{235}U/^{238}U$ ratio of ca. 1200. The measured lead isotope ratios were corrected for mass fractionation (0.076% per a.m.u.), blank and initial lead. Lead blanks were about 10 pg with isotope ratios of $^{208}Pb/^{204}Pb=37.5$, $^{207}Pb/^{204}Pb=15.5$ and $^{206}Pb/^{204}Pb=17.7$. The common lead composition was taken from the Stacey and Kramers (1975) growth model for a model lead with an age of 320 Ma.

The calculation of the $^{206}Pb/^{238}U$- and $^{207}Pb/^{235}U$-ratios was carried out with PbDat (Ludwig, 1988) for a confidence level of 95%. U–Pb ages were calculated using the constants proposed by Steiger and Jäger (1977) and Jaffey et al. (1971). The computer software Isoplot 3.0 (Ludwig, 2003) was used for regression and visualization of the results.

A sample of the Hauzenberg granodiorite was collected from the quarry Schachet (Hauzenberg) at the southern margin of the pluton (Fig. 2). Zircon ages of the Hauzenberg granodiorite where obtained using

Table 1
U–Pb analytical data for zircon and monazite of the Hauzenberg granite II (Kirchstein)

| ID[a] | Weight | U | $Pb_r$ | $Pb_i$ | $^{206}Pb/^{204}Pb$ | $^{207}Pb/^{235}U$ | $^{206}Pb/^{238}U$ | $^{207}Pb/^{206}Pb$ | Rho[b] | $^{206}Pb/^{238}U$ | $^{207}Pb/^{235}U$ | $^{207}Pb/^{206}Pb$ |
|---|---|---|---|---|---|---|---|---|---|---|---|---|
| | [μg] | [ppm] | [ppm] | [ppm] | | 2σ [%] | 2σ [%] | 2σ [%] | | [Ma] | [Ma] | [Ma] |
| Z1(1) | 107 | 392 | 18.3 | 0.28 | 4308 | 0.3630±0.48 | 0.04913±0.41 | 0.05358±0.25 | 0.86 | 309±1 | 314±2 | 353±6 |
| Z2(1) | 23 | 359 | 18.1 | 0.16 | 7254 | 0.3706±0.87 | 0.05116±0.4 | 0.05254±0.76 | 0.48 | 322±1 | 320±3 | 309±17 |
| Z3(1) | 28 | 190 | 9 | 0.05 | 11874 | 0.3684±0.86 | 0.05016±0.61 | 0.05327±0.58 | 0.74 | 316±2 | 318±3 | 340±13 |
| M1(8) | 10 | 6850 | 1142.2 | 16.9 | 1290 | 0.3666±0.75 | 0.04990±0.69 | 0.05328±0.28 | 0.93 | 314±2 | 317±2 | 341±6 |
| M2(6) | <10 | 3851 | 727.5 | 13.6 | 950 | 0.3821±2.17 | 0.05235±2.17 | 0.05293±0.14 | 0.99 | 329±7 | 329±7 | 326±3 |
| M3(6) | <10 | 5864 | 946.9 | 38.2 | 508 | 0.3697±0.46 | 0.05061±0.4 | 0.05298±0.21 | 0.89 | 318±1 | 319±1 | 328±5 |
| M4(6) | <10 | 3908 | 613.8 | 12.5 | 1030 | 0.3750±0.38 | 0.05121±0.34 | 0.05311±0.16 | 0.91 | 322±1 | 323±1 | 334±4 |

[a] Z = zircon, M = monazite. Bracketed numbers indicate number of grains in fraction. All zircons were air-abraded.
[b] Correlation coefficient of ($^{206}Pb/^{238}Pb$) / ($^{207}Pb/^{235}U$).

the zircon evaporation technique (Kober, 1986, 1987) and measurements were performed at Tuebingen University. The analytical technique is described in detail in Siebel et al. (2003). Pb isotopes were dynamically measured in a mass sequence of 206-207-208-204-206-207 in ion counting mode. Common lead correction was performed using the method of Cocherie et al. (1992). A single grain Pb–Pb age was calculated from the mean of the individual $^{207}Pb/^{206}Pb$ ratios. During Pb evaporation analyses of the granodiorite sample, five out of twelve grains turned out to be free of inherited older core components. For these grains the weighted average was calculated according to Ludwig (2003).

To determine the intrusion depth of the Hauzenberg granitoids, igneous white micas of samples from the Kirchstein quarry and from a granitic apophysis at the southern pluton (locality Taxberg, Fig. 2) were analyzed by electron microprobe (Jeol Superprobe JXA8900 at Frankfurt University). The spectrometers were calibrated with natural and synthetic silicate and oxide standards. The acceleration voltage was set at 20 kV, the beam current was kept low between 9 and 15 nA, and the beam itself was defocused (5 to 10 μm, depending on grain size) to avoid thermal destruction of the analyzed mica grains.

## 4. Results

### 4.1. Geochronology

The U–Pb data of zircon and monazite from the Hauzenberg granite II are listed in Table 1. Table 2 contains zircon evaporation data obtained from zircons of the Hauzenberg granodiorite.

#### 4.1.1. CL investigations and Pb-loss

Although diffusion of Pb, U and Th in zircon and monazite is known to be sluggish at temperatures <900 °C (Lee et al., 1997; Cherniak and Watson, 2001,

Table 2
$^{207}Pb/^{206}Pb$ evaporation data for single zircons from Hauzenberg granodiorite (Schachet)

| Sample | Number[a] | $^{204}Pb/^{206}Pb$ | $^{206}Pb^*/^{208}Pb^*$ | Th[b]/U | $^{207}Pb^{*c}/^{206}Pb^*$ | Age (Ma) | Error[d] (Ma) |
|---|---|---|---|---|---|---|---|
| Hz 7 | 258 | 0.000121 | 48 | 0.07 | 0.052745±0.000037 | 317.9 | 2.8 |
| Hz 8 | 173 | 0.000250 | 11 | 0.30 | 0.052900±0.000060 | 324.5 | 3.5 |
| Hz 11 | 296 | 0.000167 | 14 | 0.23 | 0.052697±0.000033 | 315.8 | 2.7 |
| Hz 12 | 326 | 0.000078 | 13 | 0.24 | 0.052683±0.000033 | 315.2 | 2.7 |
| Hz 13 | 349 | 0.000918 | 5.6 | 0.56 | 0.052859±0.000044 | 322.8 | 3.0 |
| **Weighted avg.** | | | | | | 318.6 | 4.1 |

[a] Number of measured $^{207}Pb/^{206}Pb$ isotope ratios per grain.
[b] Model ratio calculated from $^{208}Pb^*/^{206}Pb^*$ ratio and age of the sample; *=radiogenic lead.
[c] errors are $2\sigma_{measured}$.
[d] Error calculated using following formulae: $\sqrt{(2\sigma/\sqrt{n})^2+\Delta f^2}$, where $n$ is the number of measured $^{207}Pb/^{206}Pb$ isotope ratios, $2\sigma$ is the 2-sigma standard error of the Gaussian frequency distribution function and $\Delta f$ is an assumed uncertainty of the measured $^{207}Pb/^{206}Pb$ ratio of 0.1%.

2004), true lead loss of zircon may appear under chemical and physical processes that modify or destruct the zircon lattice, such as recrystallization, self-annealing, thermal expansion, fracturing, radiation damage and fluid alteration or leaching. During our studies it became evident that numerous zircons have inherited cores and some are fractured (Fig. 3). Inheritance is consistent with calculated melt temperatures determined with the Zr-saturation thermometer of Watson and Harrison (1983) all of which are below 800 °C in case of the Hauzenberg II granite. Under these circumstances even older monazites might have survived the melt-building process. Numerous zircons had to be abandoned due to inheritance and related discordancy. Pb-loss affected monazite fraction M1 and zircon grains Z1 and Z3 from the Hauzenberg granite II (Table 1, Fig. 4). Monazite fractions M3 and M4 yield nearly concordant data points (Fig. 4).

Due to CL and BSI investigations of representive zircons (Fig. 3), it is believed that some Pb-loss is related to hydrothermal leaching and weathering. Continuous Pb-loss during uplift and weathering appears even more likely, as it already has been recognized in case of granitoids from the Bavarian Forest (Siebel et al., 2006).

Since cathodoluminescence (CL) intensity of zircon depends on structural factors, such as crystallinity (Nasdala et al., 2002) and the abundance of trace elements (Benisek and Finger, 1993; Hanchar and Miller, 1993; Kempe et al., 2000), it may help to interpret discordant U–Pb zircon ages. Normally emission decreases with increasing U and Y (e.g. Hanchar and Miller, 1993). Radioactive decay of U and Th reduces the CL emission of zircon and may cause metamictization. Although metamictization cannot occur when temperatures are permanently high enough to allow self-annealing of zircon, rapid heating of prior metamict zircon may cause Pb-loss (Mezger and Krogstad, 1997). The CL images of zircons from the Hauzenberg granite II reveal inclusion-rich partially resorbed cores, oscillatory zoning and dark outer rims (Fig. 3a–c). The late darker growth zones show straight crystal faces and zoning, typically found in magmatic zircons. Consequently heating of metamict zircon cannot be held responsible to have caused Pb-loss. CL images of zircons of the Hauzenberg granodiorite (Fig. 3d–g) sample from the Schachet quarry are comparable to those from Hauzenberg II granite. Fig. 3d and f show grains which are related to one-episodic magmatism, whereas those in Fig. 3e and g include inherited cores. In case of Fig. 3g the grain shows light seams around a corroded core.

The backscatter images (Fig. 3a–c) reveal some fractures in zircons from the Hauzenberg granite II. From CL images (Fig. 3d and f) it is evident that zircons from the Hauzenberg granodiorite are fractured as well. Although the fracture density is not high, outer growth zones were likely subdued to isotopic exchange between crystal and fluid leading to Pb-loss by leaching. Since the fracture density is low, similar zones in the dated grains could have survived air-abrasion. In some cases changes of the chemical composition along the fractures are obvious, as is indicated by light coloured crystal zones occurring near fractures in backscatter images of Fig. 3c and CL images as well (Fig. 3d, g). Thus Pb-loss is most likely resulting from hydrothermal leaching along fractures. The negative intercept of the calculated discordia (see below, Fig. 4b) indicates that this process did not have the character of a geological event, but was continuous.

#### 4.1.2. U–Pb and Pb–Pb age data

Ten single zircons and five monazite fractions were separated and analyzed from the *Hauzenberg granite II*. Only three zircon analyses and four monazite fractions are discussed here. The remaining analyses were affected by inheritance. Due to their high uranium contents (>>100 ppm) and different ages of the inherited material, they were not suitable to calculate lower concordia intercept ages (Mezger and Krogstad, 1997). The zircons Z1 and Z3 are slightly discordant in the concordia diagram (Fig. 4a), but plot close to the concordia, between 310 and 323 Ma. Zircon Z2 is concordant with a $^{207}Pb/^{235}U$ age of 320±3 Ma. The uranium content of the monazite fractions varies from 3851 to 6850 ppm. The $^{206}Pb/^{204}Pb$ ratio ranges from 508 to 1290. All fractions are plotting close to the concordia between 318 and 330 Ma. The concordant monazite fraction M2 has a large uncertainty, but within error, overlaps with zircon Z2 (Fig. 4a). Monazite

Fig. 3. Cathodoluminescense (CL) and corresponding backscatter images (BSI) of zircon. Images a–c are zircons from Hauzenberg granite II, d–g from Hauzenberg granodiorite. The CL images reveal that most zircons have an inherited core (exceptions: d, f). Incompatible elements, which cause darker CL, are enriched in the outer growth zones (Benisek and Finger, 1993). These growth zones are fine-scale oscillating and interpreted to reflect the magmatic stage. In image a) (CL) two zones were marked with *X* and *Y*. There, the core is delimited by a distinct discordance towards the outer zone, the latter being enriched with incompatible elements. Inherited cores are rich in inclusions (b, c, e) and show embayments (a, b, c, g) that could result from resorption (Hanchar and Miller, 1993). Euhedral rims indicate final growth in melt. Chemical variations along fractures can be recognized by variations in brightness of both, CL and BS images (e.g. a, c, g).

fractions M3 and M4 are subconcordant (Fig. 4a) and are plotting between ca. 319 and ca. 323 Ma. The fact that monazite and zircon give similar results points to simultaneous isotopic closure of both mineral systems. Tracing a discordia through subconcordant and discordant zircon and monazite fractions could be valid, if Pb-

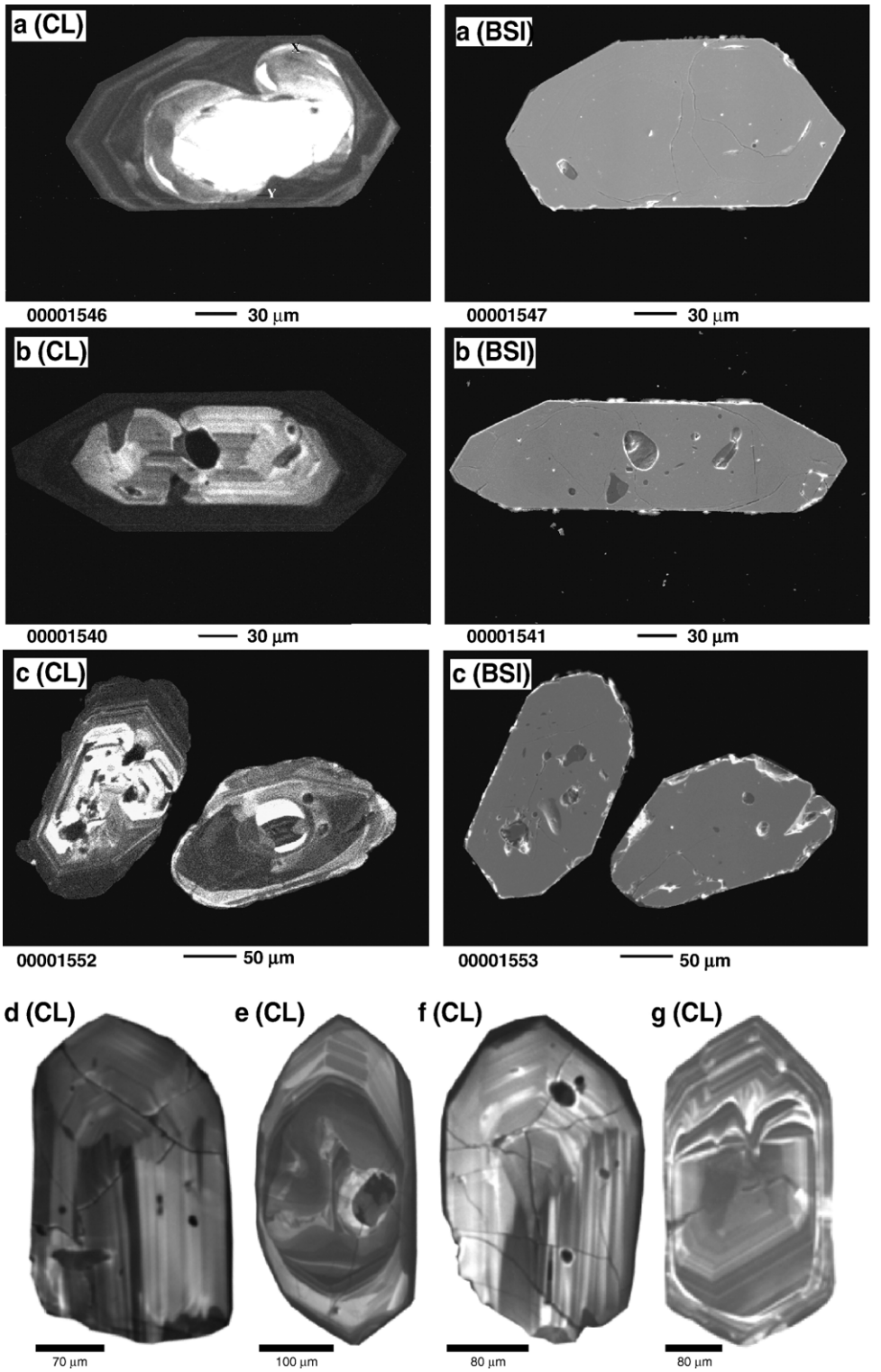

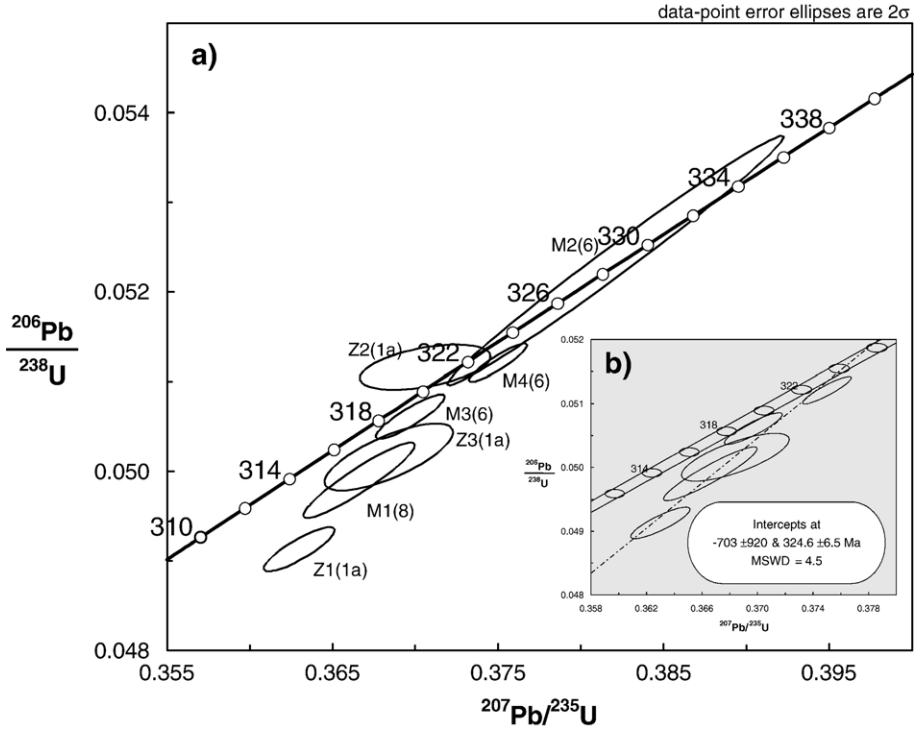


Fig. 4. a) Concordia diagram of the analyzed zircon and monazite-fractions of Hauzenberg granite II, Z = zircon, M = monazite, all zircons were air-abraded, bracketed numbers indicate number of grains in fraction. As it is shown in b) sub- and discordant minerals can be used to trace a discordia that has a similar upper intercept age as indicated by grain Z2 and fraction M2.

loss occurred approximately coeval for all grains. Regression results in an upper intercept age of 325 ± 7 Ma (Fig. 4b). However, the high MSWD of 4.5 and the negative intercept of −703 ± 920 Ma indicate that one-episodic Pb-loss is not sufficient to cause the discordances. The concordant age of zircon Z2 (i.e. ca. 320 Ma) is interpreted to reflect the emplacement of the Hauzenberg granite II.

Twelve zircons extracted from the *Hauzenberg granodiorite* were analysed by the Pb evaporation method. Seven analyses were not taken into account due to the contribution of lead from older cores even at the lowest temperature evaporation steps.

For five zircon grains, data of which are compiled in Table 2, no shift in $^{207}Pb/^{206}Pb$ ages between the different temperature heating steps was detectable and therefore these grains are unlikely to be affected by inheritance. Three of the five zircons (Hz 7, Hz 11, Hz 12) yielded $^{207}Pb–^{206}Pb$ evaporation ages below 320 Ma (Fig. 5). Zircon Hz 13 and Hz 8 are substantially older. However, only zircon Hz 8 is not overlapping the younger ages in error. As the age of zircon Hz 8 relies upon a low number of Pb–Pb ratios, its significance is limited. The weighted average of 318.6 ± 4.1 Ma (Fig. 5) is considered as the age of emplacement.

### 4.2. Geobarometry

The Si content of white mica generally increases with pressure (Velde, 1965, 1967; Massonne and Schreyer, 1987; Massonne and Szpurka, 1997). For the paragenesis kfs + qtz + phl + $H_2O$ (mineral abbreviations according to Kretz, 1983; cel = celadonite), which is present in the investigated granite samples, the phengite content of primary magmatic white mica is a function of the activities of the aforementioned phases and muscovite (Massonne and Schreyer, 1987).

The temperature during growth of magmatic muscovite can be constrained considering literature data that include solidus temperatures in the haplogranite system. As the bulk sample of the investigated Hauzenberg granite II (Kirchstein quarry) (Fig. 6a and c) contains cordierite and sillimanite, we have chosen a thermodynamically recalculated solidus diagram of Johannes and Holtz (1996) that includes a specific correction for crd-sil-bearing granites: the solidus is shifted to slightly

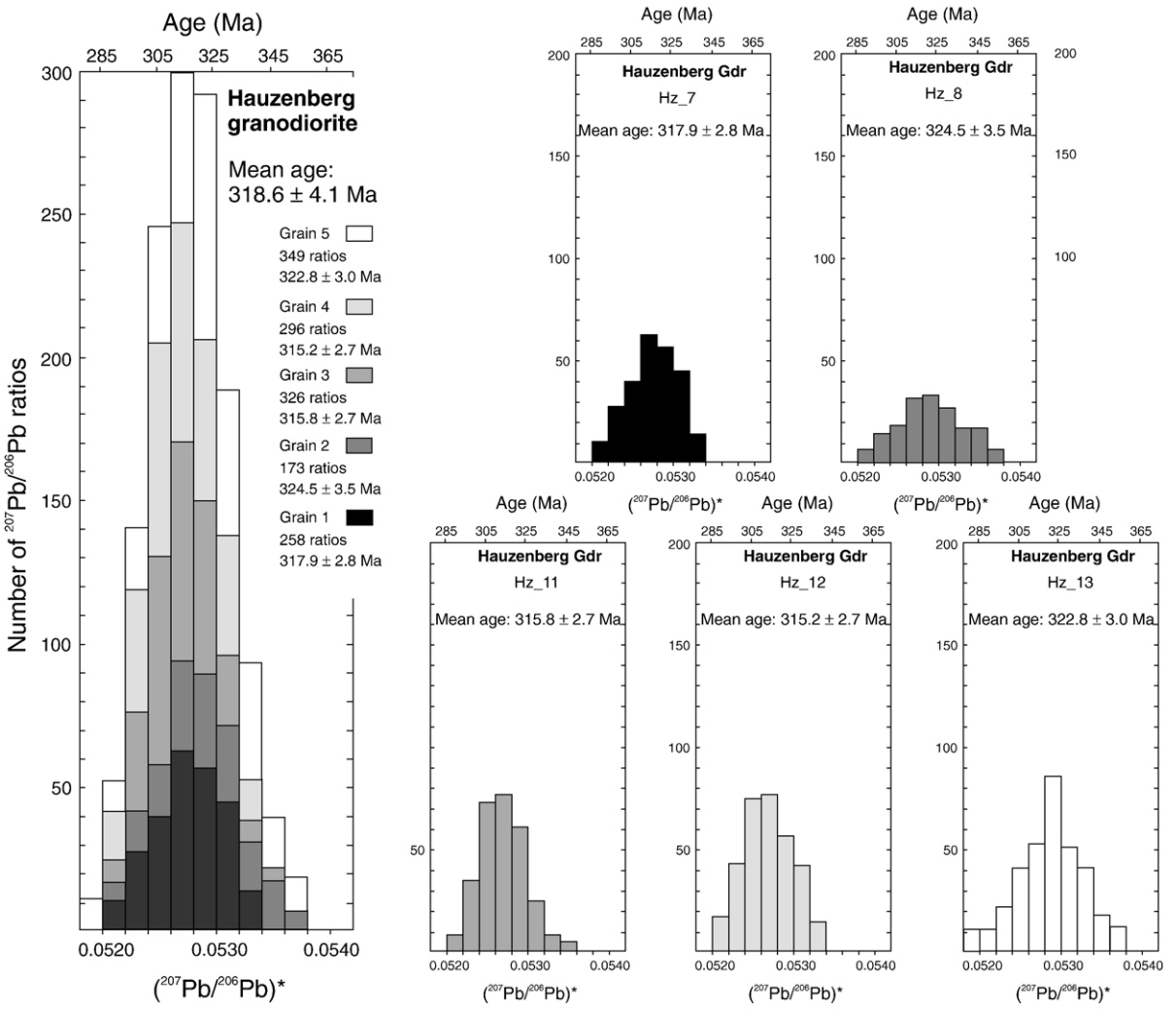


Fig. 5. Histograms showing the frequency distribution of radiogenic $^{207}Pb/^{206}Pb$-ratios obtained by evaporation of five zircons of the Hauzenberg granodiorite. From combination of the single-grain data a weighted mean age is calculated.

lower (~20 °C) temperatures in comparison with other sources (e.g. Keppler, 1989). The granite dyke from quarry Taxberg does not bear cordierite, but sillimanite. However, the aforementioned solidus appears to be applicable, too, as abundant muscovite points to a water-saturated melt.

In both samples magmatic crystallization of biotite and the oldest generation of white mica is evident (Fig. 6c, d). Thus the crystallization temperature of the analyzed white micas must have exceeded the solidus temperature of the corresponding melts. The intersection of the Si isopleth determined and the solidus then yields a minimum pressure for the partially molten granites (Fig. 7). However, it has to be emphasized that pressures obtained from phengite barometry may vary depending on the thermodynamical dataset used (e.g. Simpson et al., 2000).

*4.2.1. Hauzenberg granite II*

Within the medium-grained, hypidiomorphic-granular sample (Fig. 6a, g) three generations of white mica (ms) are distinguishable. Hypidiomorphic ms1 – the magmatic type – shows inclusions of monazite and zircon (Fig. 6d) and pleochroitic haloes, although they are not as frequent as in biotite (Fig. 6c). The grain size of ms1 is relatively large (up to 1 cm). Crystallographically orientated pairs of ms1 and biotite have been found in several cases (Fig. 6d). The critical paragenesis for phengite barometry is given for ms1 of the matrix (Fig. 6g). Ms1 grains that are included in feldspar may reflect earlier growth stages (Fig. 6h). Anhedral ms2 formed below the solidus and grew mainly within cracks of kfs. It is possible, that the growth of ms2 (Fig. 6f) was supported by potassium-rich fluids that infiltrated the

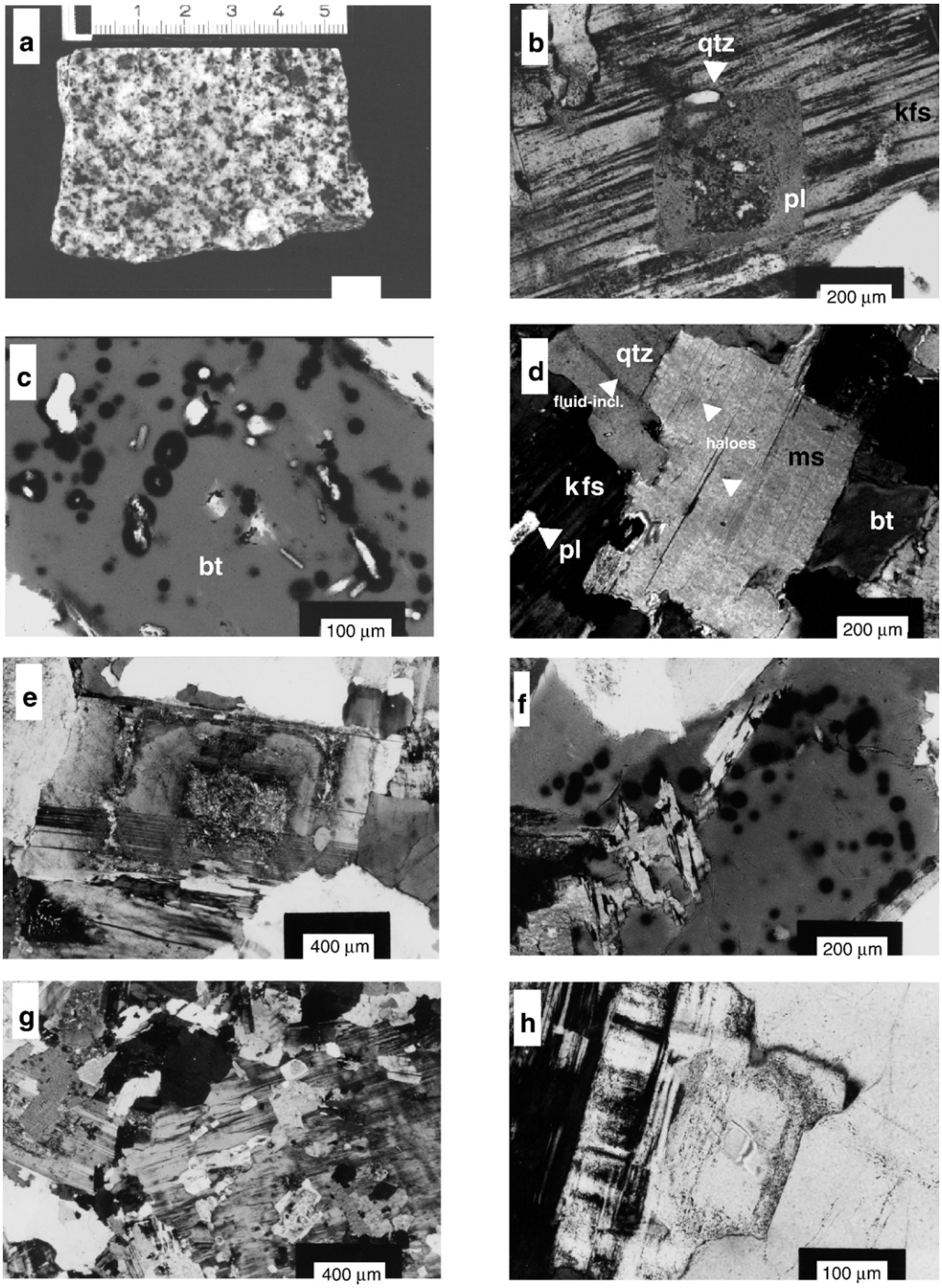


Fig. 6. Mesoscopic and microscopic views (crossed Nicols) of the Hauzenberg granite II: (a) Handspecimen. (b) Magmatic plagioclase (pl), appearing as inclusion inside perthitic K-feldspar (kfs). The contact to a small quartz-grain ("Tropfenquartz") shows anomalous interference colors, possibly resulting from transformation to α-quartz. (c) biotite (bt) commonly bears many inclusions of heavy minerals. (d) Magmatic muscovite (ms1) is characterized by pleochroitic haloes around heavy minerals and idio- to subidiomorphic crystal habitus. (e) Oscillatory zoned plagioclase, showing two main phases of growth and overgrowing magmatic bt. The concave contour of the inner core suggests that older grains became dissolved either by an increase of melt temperature or by changes in chemical composition. The an-rich core region is replaced by fine-grained sericite (ms3). (f) Irregularly shaped ms that formed below solidus-temperature (ms2). (g) The magmatic assemblage appears as inclusions in perthitic kfs. (h) Magmatic ms flake (ms1) that has been overgrown by feldspar.

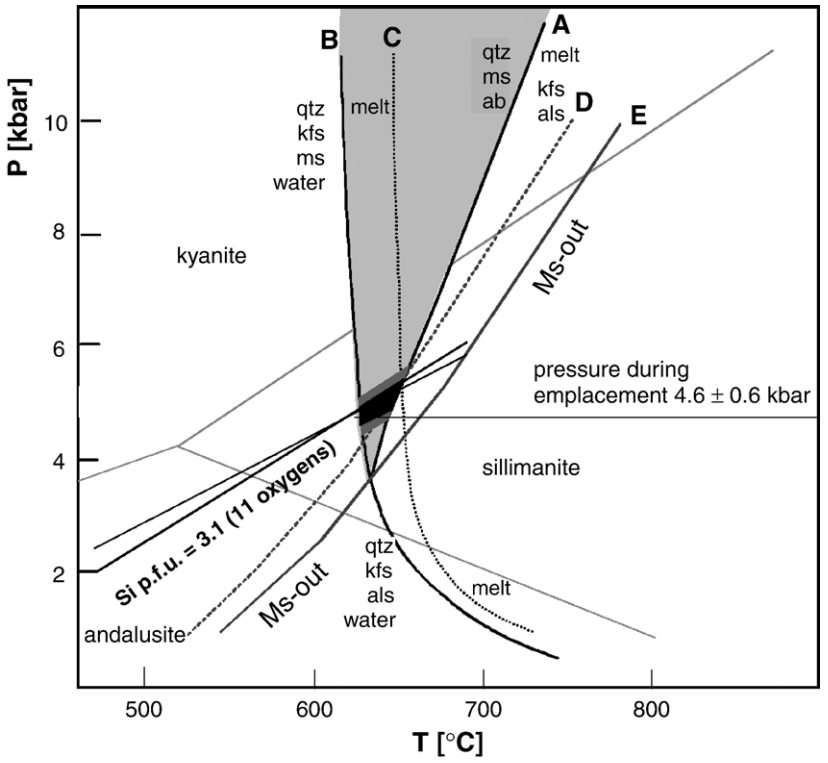


Fig. 7. Constraints on the emplacement depth of the Hauzenberg granite II by phengite barometry. Crystallization of muscovite (ms) from melt is limited to the shaded field. In case of the Hauzenberg granite the black ($1\sigma$) and dark grey ($2\sigma$) fields mark the $P$–$T$-window where magmatic ms crystallizes. Reactions after Johannes and Holtz (1996) for water activities of 1 and 0.8, respectively. 3.1 Si-Isopleth after Massonne and Schreyer (1987, lower slope) and Massonne and Szpurka (1997, steeper slope), ky-and-sil triple point after Pattison (1992).

cooling granite. Potassium became available during the formation of chlorite at the expense of biotite. As the formation temperature for ms2 is difficult to constrain and its grain-size is often too small to provide adequate microprobe data, it has not been considered for phengite barometry. However, a very different composition is recognized by electron microprobe analyses (Table 3) and indicates isobaric cooling. Ms3 is a hydrothermally formed sericite, which grew at the expense of K-feldspar and plagioclase (Fig. 6e). The critical paragenesis for phengite barometry was not stable while these late micas developed and the grains are too tiny to be measured by electron microprobe analyses.

A weak chemical zonation of ms1 exists: Si contents are highest in the core and decrease gradually towards the rim (Fig. 8). The Si enriched cores could reflect crystallites that predate the final emplacement. However, resorption of magmatic plagioclase as shown in Fig. 6e is indicative for compositional or thermal variations during magma crystallization, which also might have occurred during white mica growth. The Si contents of ms1 range from 3.05 (ms1 inclusion in kalifeldspar) to 3.12 per formula unit (p.f.u) (Table 3), with a mean value at 3.08±0.02 p.f.u.. The shape of the frequency distribution is asymmetric (Fig. 9).

The fluorine content of the white micas varies between 0.2 and 0.7 wt.%. Cr, Mn and Ca appear in traces only and the paragonite component is generally low (Table 3), but points to igneous origin ($X_{Na}>0.06$; Monier et al., 1984). The Ti content of ms1, which might be used as chemical criterion for a magmatic origin of white mica (Speer, 1984), varies between 0.02 and 0.05 cations p.f.u. for matrix grains, but is much lower for grains included in feldspar.

Applying the Si-in-phengite barometer to igneous white mica results in an emplacement pressure of 4.6± 0.3 kbar corresponding to a minimum intrusion depth of 16–18 km, assuming a density of the hanging-wall rocks of 2.7–2.8 g/cm$^3$ (Fig. 7). As the isopleths published by Massonne and Schreyer (1987) and Massonne and Szpurka (1997) intersect at the solidus (Fig. 7), the result does not depend on which publication is considered. However, an error arises from uncertainties in assigning crystallization temperatures for muscovite (i. e. assessment of the granitic solidus). The error can be bracketed as primary magmatic muscovite, andalusite, sillimanite and

Table 3
Electron microprobe analyses of magmatic white micas

| ID[a] wt.% ox.\ generation | Tax50 Ms 1 | Tax65 Ms 1 | Tax72 Ms 1 | Tax54 Ms 1 | II1-22 Ms 2 | II1-48 Ms 1 | II2-38 Ms 1 | II2-39 Ms 1 | II2-40 Ms 1 | II2-42 Ms 1 | II2-47 Ms 1 | II2-48 Ms 1 | II2-49 Ms 1 | II2-50 Ms 1 | II2-52 Ms 1[b] | II2-58 Ms 1[b] |
|---|---|---|---|---|---|---|---|---|---|---|---|---|---|---|---|---|
| $SiO_2$ | 45.46 | 44.69 | 45.51 | 45.56 | 44.95 | 45.37 | 46.60 | 47.05 | 46.26 | 45.61 | 46.26 | 46.14 | 46.12 | 46.10 | 45.39 | 46.25 |
| $TiO_2$ | 0.19 | 1.34 | 0.66 | 0.52 | 0.39 | 0.73 | 0.81 | 0.52 | 0.61 | 0.46 | 0.50 | 0.46 | 0.56 | 0.55 | 0.00 | 0.10 |
| $Al_2O_3$ | 35.25 | 33.95 | 34.70 | 35.50 | 30.96 | 34.71 | 34.06 | 33.56 | 34.01 | 34.05 | 34.82 | 34.30 | 33.98 | 34.42 | 36.68 | 35.20 |
| $Cr_2O_3$ | 0.00 | 0.00 | 0.00 | 0.00 | 0.00 | 0.01 | 0.01 | 0.00 | 0.00 | 0.00 | 0.00 | 0.00 | 0.00 | 0.00 | 0.00 | 0.00 |
| FeO | 1.19 | 1.19 | 1.10 | 1.03 | 2.66 | 1.56 | 1.70 | 2.02 | 1.74 | 1.80 | 1.71 | 1.70 | 1.76 | 1.75 | 0.35 | 1.29 |
| MnO | 0.03 | 0.01 | 0.00 | 0.01 | 0.05 | 0.03 | 0.04 | 0.04 | 0.02 | 0.02 | 0.02 | 0.02 | 0.01 | 0.01 | 0.00 | 0.01 |
| MgO | 0.59 | 0.57 | 0.58 | 0.51 | 1.42 | 0.64 | 0.76 | 0.98 | 0.71 | 0.69 | 0.71 | 0.69 | 0.73 | 0.74 | 0.04 | 0.39 |
| CaO | 0.03 | 0.06 | 0.01 | 0.01 | 0.06 | 0.00 | 0.01 | 0.00 | 0.02 | 0.06 | 0.02 | 0.01 | 0.01 | 0.00 | 0.01 | 0.00 |
| NaO | 0.59 | 0.59 | 0.49 | 0.42 | 0.25 | 0.58 | 0.55 | 0.29 | 0.70 | 0.71 | 0.86 | 0.81 | 0.75 | 0.73 | 0.76 | 0.55 |
| $K_2O$ | 10.03 | 9.85 | 10.42 | 10.23 | 10.36 | 10.24 | 10.62 | 11.01 | 10.23 | 9.88 | 10.05 | 10.05 | 10.22 | 10.25 | 10.31 | 10.76 |
| F | – | – | – | – | – | – | 0.63 | 0.46 | 0.53 | 0.53 | 0.58 | 0.58 | 0.71 | 0.57 | 0.17 | 0.27 |
| ∑ (wt.%) | 93.36 | 92.25 | 93.47 | 93.79 | 91.1 | 93.87 | 95.79 | 95.93 | 94.83 | 93.81 | 95.53 | 94.76 | 94.85 | 95.12 | 93.71 | 94.82 |
| Cation proportions (1 formula unit = 11 O) | | | | | | | | | | | | | | | | |
| Si | 3.078 | 3.068 | 3.083 | 3.068 | 3.159 | 3.068 | 3.103 | 3.132 | 3.105 | 3.086 | 3.078 | 3.095 | 3.097 | 3.086 | 3.053 | 3.097 |
| Al | 0.922 | 0.932 | 0.917 | 0.932 | 0.841 | 0.932 | 0.897 | 0.868 | 0.895 | 0.914 | 0.922 | 0.905 | 0.903 | 0.914 | 0.947 | 0.903 |
| sum *T* | 4.000 | 4.000 | 4.000 | 4.000 | 4.000 | 4.000 | 4.000 | 4.000 | 4.000 | 4.000 | 4.000 | 4.000 | 4.000 | 4.000 | 4.000 | 4.000 |
| Al | 1.891 | 1.815 | 1.853 | 1.886 | 1.724 | 1.835 | 1.773 | 1.765 | 1.795 | 1.801 | 1.810 | 1.807 | 1.787 | 1.801 | 1.961 | 1.875 |
| Fe | 0.067 | 0.068 | 0.063 | 0.058 | 0.156 | 0.088 | 0.094 | 0.113 | 0.098 | 0.102 | 0.095 | 0.095 | 0.099 | 0.098 | 0.019 | 0.072 |
| Mg | 0.059 | 0.059 | 0.058 | 0.051 | 0.149 | 0.064 | 0.076 | 0.098 | 0.071 | 0.074 | 0.070 | 0.069 | 0.073 | 0.074 | 0.040 | 0.039 |
| Ti | 0.009 | 0.069 | 0.034 | 0.026 | 0.020 | 0.037 | 0.041 | 0.026 | 0.031 | 0.023 | 0.025 | 0.023 | 0.028 | 0.027 | 0.000 | 0.005 |
| Mn | 0.002 | 0.001 | 0.000 | 0.001 | 0.003 | 0.001 | 0.002 | 0.002 | 0.001 | 0.001 | 0.001 | 0.001 | 0.001 | 0.000 | 0.001 | 0.001 |
| sum *M* | 2.028 | 2.012 | 2.008 | 2.022 | 2.052 | 2.025 | 1.986 | 2.004 | 1.996 | 2.001 | 2.001 | 1.995 | 1.988 | 2.000 | 2.021 | 1.992 |
| K | 0.866 | 0.863 | 0.901 | 0.879 | 0.929 | 0.883 | 0.901 | 0.935 | 0.875 | 0.866 | 0.853 | 0.860 | 0.875 | 0.875 | 0.885 | 0.919 |
| Na | 0.078 | 0.079 | 0.065 | 0.054 | 0.034 | 0.076 | 0.072 | 0.038 | 0.090 | 0.099 | 0.111 | 0.105 | 0.098 | 0.094 | 0.099 | 0.071 |
| sum *A* | 0.946 | 0.942 | 0.966 | 0.933 | 0.963 | 0.959 | 0.973 | 0.973 | 0.965 | 0.965 | 0.964 | 0.965 | 0.973 | 0.969 | 0.984 | 0.990 |

[a] Prefix II=Hauzenberg granite II/Kirchstein; prefix Tax = granite dyke/Taxberg.
[b] Inclusion in magmatic feldspar.

β-Quartz (see also Fig. 6b) coexist within the Hauzenberg granite, which is only possible under very distinct temperatures (Clarke et al., 2005). It amounts ±0.6 kbar.

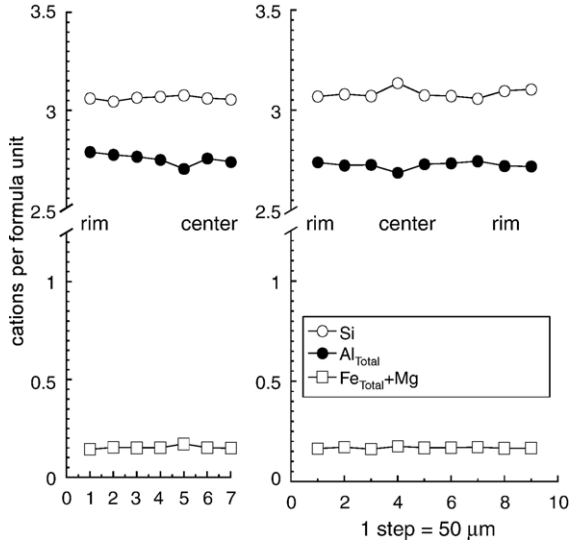


Fig. 8. Zonation patterns of igneous muscovite in Hauzenberg granite II.

*4.2.2. Granite dyke*

The analysed prekinematic fine-grained granitic dyke, which is located about 1 km S of the main pluton and has a thickness of 2–3 m, yields Si contents of 3.07–3.12 (e.g. Table 3) and a mean value of 3.08±0.02 for magmatic white micas ($n$=15). Mica fishes and undeformed mica flakes do not show compositional differences. Feldspar recrystallization and the occurrence of chessboard quartz prove that the dyke became sheared at temperatures above 500 °C. As the main pluton is free of ductile shear zones, the dyke must be older than the Hauzenberg granites. The composition of magmatic phengite inside the granitic dyke corresponds to very similar pressures and thus indicates a lack of substantial uplift between dyke-emplacement and the main magmatic activity.

## 5. Discussion and conclusions

*5.1. Ages and intrusion levels reported from the Hauzenberg pluton and adjacent plutons*

The Hauzenberg granite II intruded at mid-crustal levels (16–18 km) in middle Carboniferous times. The

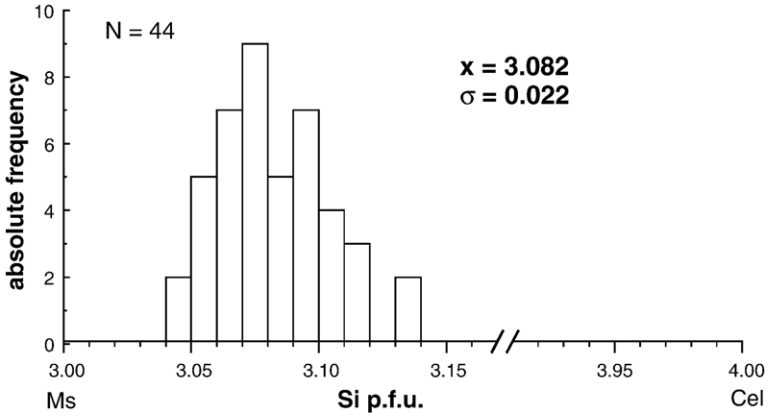


Fig. 9. Frequency distribution of measured Si in white micas from Hauzenberg granite II.

concordant zircon age at 320±3 Ma (Hauzenberg granite II) as well as the mean Pb–Pb age of 318.6± 4.1 (Hauzenberg granodiorite) are interpreted as the best approximation for the time of melt emplacement. The intrusion depth given above is further supported by petrological constraints (Olbrich, 1985) and by a similar emplacement level of the Taxberg granite dyke south of the massif. Sinistrally sheared granite dykes from a quarry near Saunstein, yielded substantially higher Si values, but are slightly older based on preliminary U–Pd age data (Galadí-Enríquez et al., 2006, Galadí-Enriquez, pers. comm.). These data might indicate a period of exhumation and cooling prior to the intrusion of the larger granite plutons.

Al-in-hornblende barometry of diorites occurring to the south of the Saldenburg granite (Fürstenstein complex) yields pressures of 4.2–4.7 kbar (Dietl et al., 2005). According to Dietl et al. (2005) the composition of the amphiboles was reset due to the emplacement of the Saldenburg granite. In agreement with other barometric data for the Saldenburg and Hauzenberg granite (Massonne, 1984), it then indicates a similar emplacement depth of the latter.

The U–Pb age of the Hauzenberg granite II and the Pb–Pb age of the Hauzenberg granodiorite show consistency with U–Pb ages of adjacent granites (Table 4, Figs. 10 and 11). The Tittling granite of the Fürstenstein complex (Troll, 1964, 1967a) yielded U–Pb and Pb–Pb zircon ages ranging from 323 to 321 Ma (Chen and Siebel, 2004). Zircons from diorites of the Fürstenstein complex are significantly older (334–331 Ma). However, titanites from these diorites yield U–Pb ages of 321±4 Ma, suggesting thermal resetting or crystallization of titanite to result from the emplacement of the Tittling granite (Chen and Siebel, 2004). Granites at the Bavarian Lode ("Pfahl") shear zone (Rinchnach, Patersdorf) gave mean Pb–Pb zircon ages of 321–329 Ma (Siebel et al., 2006) and two concordant zircon fractions of the adjacent granodiorites yielded 325±3 and 326±3 Ma, respectively. The zircon fractions that came from the Rinchnach and Patersdorf granites all plot on a discordia that has an upper intercept age of 330±13 Ma (MSWD=11.1). Although this discordia is not well defined, the large distance of ca. 20 km between the aforementioned granites suggests that Pb-loss is related to an extensive geological process: Siebel et al. (2006) suggest Pb-removal during recent weathering or continuous removal during uplift. The sub- and discordance of zircons presented in this paper are interpreted to result from similar processes.

Ages >330 Ma seem to be restricted to more basic types of intrusive rocks (Table 4). The synkinematic granodioritic Palites (Frentzel, 1911) yielded 334±3 Ma Pb–Pb zircon evaporation ages, which date the earliest activities along the Bavarian Lode shear zone (Siebel et al., 2005a), thereby refining Ordovician Rb–Sr whole rock ages by Christinas et al. (1991a). The Palite body is crosscut by synkinematic granite dykes that yielded slightly younger upper discordia intercept ages (Siebel et al., 2005a).

The ~320 Ma ages have also been reported from rocks of the northwestern part of the Bavarian Forest. Grauert et al. (1974) obtained U–Pb zircon and monazite multi-grain ages of 320 Ma for the Kollnburg granodiorite (as defined by List, 1969). The Oedwies granodiorite yielded a Rb–Sr whole rock-age of 331±9 Ma but significantly younger U–Pb zircon ages of 320 and 318 Ma (Grauert et al., 1974; Propach et al., 1991, 2000).

### 5.2. Subsequent cooling and minor magmatic events

Rb–Sr and K–Ar cooling ages of white mica and biotite of the Hauzenberg granitoids are between 280

Table 4
Compilation of radiometric ages from late-Variscan granites, SW Bohemian Massif

| Rock type | Discordant U–Pb ages | U–Pb | | | | Ref. | Pb–Pb | Ref. | Rb–Sr | (Ref.) | | Sr(i) | Ref. | K–Ar | | | Ref. | Ar–Ar | Ref. |
|---|---|---|---|---|---|---|---|---|---|---|---|---|---|---|---|---|---|---|---|
| | | zrn | mnz | ttn | other | | zrn | | ms | bt | wr; other | | | ms | bt | hbl | | | |
| *Bavarian Forest* | | | | | | | | | | | | | | | | | | | |
| Kirchstein–Porphyrit | | | | | | | | | | | 302±7 (wr,bi,ap) | 0.7076±5 | *C91b* | | | | | | |
| Hauzenberg granite 2 | | 320±3 | 327±9 | | | this study | | | | | 312±6 (wr,bi,ap) | 0.7089±1 | *C91b* | | | | | | |
| Hauzenberg granite 1 | | | | | | | | | | 310±3 | | | *H67* | 313±3 | 293±3 | | *H67* | | |
| | | | | | | | | | | | | | | 284±3 | | | *H67* | | |
| Hauzenberg granodiorite | | | | | | | 318.6±4 | *this study** | | 302± 13 | | | *H67* | | 294±5 | | *H67* | | |
| | | | | | | | | | | | | | | | 284±4 | | *H67* | | |
| Saldenburg granite | | | | | | | 315±3 | *Ch04** | | | | | | 296±3 | 286±3 | | *H67* | | |
| Tittlingen granite | | | | | | | 323±1 | *Ch04** | | 312±5 | | | *DS62* | | | | | | |
| Eberhardsreuth granite | | | | | | | 314±2 | *Ch04** | | | | | | | | | | | |
| Fürstenstein diorites | | | | 321±4 | | | 334±1 | *Ch04** | | | 320±3 (kfs, MSWD=18) | | *S05b* | | | | | | |
| Platte Granite (Gurlarn) | | | 311±2 | | | *P00* | | | | | | | | | | | | | |
| Metten granite | | | | | | | | | 315±5 | | | | *H67* | 303±6 | | | *H67* | | |
| Neustift granite | | | | | | | | | | 322±5 | | | *DS62* | | | | | | |
| Metabasites (Passau) | | 313±5 (rim, SHRIMP) | | | | *T04* | | | | | | | | | | | | | |
| Metarhyolithes (Passau) | | 319±5 (rim, SHRIMP) | | | | *T04* | | | | | | | | | | | | | |
| Quartz dyke ("Pfahl") | | | | | | | | | | | 247±9(qtz) | 0.7133±4 | *Horn86* | | | | | | |
| Palite (different sites) | | 327–342 | | | | *S05* | 334±3 | *S05* | | | 474±18 | 0.7051±11 | *C91a* | | | | | | |
| granitic dykes in Palite | 322±5 (UCI, Pb-loss) | | | | | *S05* | | | | | | | | | | | | 287(ms) | B95 (Austria) |
| | 331±9 (UCI, Pb-loss) | | | | | *S05* | | | | | | | | | | | | | |
| Palite (5 sites) | | | | | | | | | | 310±7 (bt, ap) | | | *C91a, K89* | | | | | | |
| Flasergranite (in Palite) | | | | | | | | | 316±6 | | | | *C91a* | | | | | | |
| Pearlgneiss (Padling) | | | | | | | | | | | 312±16 | 0.7107±4 | *K89* | | | | | | |
| Granodiorite (Saunstein) | | ~325 | | 306–319 | | *S05b* | | | | | 250–323 (kfs) | | *S05b* | | | | | | |
| Granodiorites (Patersdorf) | | 325±3,326±3 | | | | *S06* | | | | | 308±5(kfs) | 0.7081–0.7086 | *S05b, S06* | | | | | | |
| Granite (Patersdorf) | 330±13 (UCI Pb-loss) | | | | | | 322±2, 323.4±1.6 | *S06* | | | | 0.706–0.7071 | *S06* | | | | | | |
| Granite (Rinchnach) | | | | | | | 329.2±2.1, 320.4±6.5 | *S06* | | | | 0.706–0.7071 | *S06* | | | | | | |
| Granite (Padling) | | | | | | | | | | | 299±10 | 0.7123±5 | *K89* | | | | | | |
| | | | | | | | | | | | 323±38 | 0.7085±10 | *K89* | | | | | | |
| Diorite (Padling) | | | | | | | | | | | 309±33 | 0.7088±9 | K89 | | | | | | |
| | | | | | | | | | | | 323±38 | 0.7085±10 | K89 | | | | | | |
| Pearlgneiss (Bischofsmais) | | 319 | | | | G74 | | | | | | | | | | | | | |
| qtz–mica diorite (Bischofsmais) | | 310 | | | | G74 | | | | | | | | | | | | | |
| Bt–Pl gneiss (Ruselabsatz) | | | 320±3 | | | *G74* | | | | 303±9 | 313±70 | 0.7131 | *G74* | | | | | | |

| | | | | | | | | | | | | | | | | | | | |
|---|---|---|---|---|---|---|---|---|---|---|---|---|---|---|---|---|---|---|---|
| Bt gneiss (Silberberg) | | | | 320±3 | | | *P00* | | | | 328±5 (model age) | | | *DS62* | | | | | |
| Bt–Crd–Sil gneiss (ECK) (different sites) | | | | 320±3 | | | *G74* | | | | 319±7 | 324±15 | | *G74* | | | | | |
| | | | | 317±3 | | | *G74* | | | | 321±9 | | | *G74* | | | | | |
| Migmatites (Bodenmais) | | | 324.5±1.5 | | 321±1 | | *Ka00* | | | | | | | | 311±2 | | 319±3 | *Ka00* | |
| Diorite dykes, Regensburger Wald | | | | | | | | | | | | 335±12 | 0.7076±3 | *KM86* | | 320±8 | | *H67* | |
| Paragranodiorite (Kollnburg; List, 1969) | | | 322 | | | | *G74* | | | | | | | | | | | | |
| Oedwies granite | | | 320 | | | | *G74* | | | | | | | | | | | | |
| Oedwies granodiorite (Irschenbach) | 1510±64 | 326±5 (LCI) | 318±2 | 318±2 | | | *P00* | | | | 311±6 | | | *P91* | | | | | |
| Oedwies granodiorite (Irschenbach) | | | 320±2 | | | | *P00* | | | | | | | | | | | | |
| Oedwies granodiorite (Irschenbach) | 1449±59 | 329±6 (LCI) | | | | | *P00* | | | | | 331±9 | 0.7092±2 | *P91* | | | | | |
| Pearlgneiss(Gossersdorf/ Irschenbach) | | | | 321±2 | | | *P00* | | | | | | | | | | | | |
| Crd–Sil–gneiss (Gossersdorf) | | | | 322±2 | | | *P00* | | | | | | | | | | | | |
| Mylonitic paragneiss (Flammried) | | | | 323±2 | | | *P00* | | | | | | | | | | | | |
| Diorites (different sites) | | | | | | | | | | | 317±8 | 311±28 | 0.7151±11 | *K89* | | | | | |
| Anatexite (Schwarzenfeld) | | | | | | | | | | | | 335±12 | 0.7076±3 | *KM86* | | | | | |
| | | | | | | | | | | | | | | | 314±12 | | | *H67* | |
| Bändergneiss (Lichtenwald) | | | | | | | | | | | 319±6 | | | *H68* | | 316±6, 325±6 | | *H67* | |
| Bt–Pl–Gneiss (Völling) | 384(LCI) | 2429 (UCI) | | | | 322(xtm) | *G89* | | | | | 320±7 (ap,pl,kfs,bt) | 0.7152±4 | *G89* | | | | | |
| Anatectic paragneiss (Völling) | 459±8(LCI) | 2372±100 (UCI) | | | | 323±1(xtm) | *G89* | | | | | | | | | | | | |
| Anatectic paragneiss (Perlbachtal) | | | | | | | | | | | 324±7 | | | *K89* | | | | | |
| Anatectic paragneiss (Perlbachtal) | | | | | | | | | | | | 436±15 | 0.7099±3 | *KM86* | | | | | |
| Anatectic paragneiss (Falkenstein) | | | | | | | | | | | | 438±17 | 0.7110±6 | *KM85* | | | | | |
| "Körnelgneis" (Reftal) | | | | | | | | | | | 321±6 | | | *H68* | | 323±8 | | *H67* | |
| Trasching granite | | | | 321±3 | | | *P00* | | | | | | | | | | | | |
| Trasching diorite | | | | | | | | | | | | | | | 320±8 | | | *H67* | |
| "Kristallgranit 1" (11 sites) | | | | | | | | | | | | 349±11 | 0.7076±5 | *KM86* | | | | | |
| "Kristallgranit 1" (Reichenbach) | | | | | | | | | 313±10 | | 317±6 | | | *H68* | 314±6 | 320±5 | | *H67* | |
| "Kristallgranit 1" (Reichenbach) | | | | | | | | | | | | 326±9(ap,pl, kfs,bt,wr | | *K89* | | | | | |
| "Kristallgranit 1" | | | ~315 | | | | *G74* | | | | | 326±6 | | *SS84* | 318±3 | 318±3 | | *H67* | |
| "Kristallgranit 1" (Frankenberg) | | | 315±4 | 317±3 | | | *P00* | | | | | | | | | | | | |
| | | | | 318±3 | | | *P00* | | | | | | | | | | | | |

(continued on next page)

Table 4 (*continued*)

| Rock type | Discordant U–Pb ages | U–Pb | | | | Ref. | Pb–Pb | Ref. | Rb–Sr | (Ref.) | | Sr(i) | Ref. | K–Ar | | | Ref. | Ar–Ar | Ref. |
|---|---|---|---|---|---|---|---|---|---|---|---|---|---|---|---|---|---|---|---|
| | | zrn | mnz | ttn | other | | zrn | | ms | bt | wr; other | | | ms | bt | hbl | | | |
| "Kristallgranit 2" | | | | | | | | | | 315±8 | 319±7 | 0.7116±5 | *K89, KM86* | | | | | | |
| *Austrian moldanubian* | | | | | | | | | | | | | | | | | | | |
| Weinsberg granites (6 sites) | | | | | | | | | | | 349±4 | 0.7064±2 | *Sc87* | | | | | | |
| Weinsberg palingenic sector | | | | | | | | | | | 328±6 | 0.7102 | *FQ92* | | | | | | |
| Weinsberg anatectic sector | | | | | | | | | | | 336±19 | 0.708 | *FQ92* | | | | | | |
| Weinsberg granite | | 316±17 | 318±4 | | 314±4 (xtm) | *QF91* | | | | | | | | | | | | | |
| Weinsberg (Grein) | | | 327±5 | | | *Fr96* | | | | | | | | | | | | | |
| Weinsberg (Altweitra) | | | 328±5 | | | *Fr96* | | | | | | | | | | | | | |
| Weinsberg (Naarntal) | | | 327±5 | | | *Fr96* | | | | | | | | | | | | | |
| Weinsberg (Langschlag) | | | 323±4 | | | *Fr96* | | | | | | | | | | | | | |
| Weinsberg (Sarleinsbach) | 529±22 (PbPb-mean age) | 345±5 | | | | *Kl01* | 355±9 | *Kl01* | | | 330±28 | 0.7081±9 | *Kl01* | | | | | | |
| Eisgarn granite | | | 327±4 | | | *FF91,Fr96* | | | | | | | | | | | | | |
| Schärding granite | | | 319±6 | | | *FF91,Fr96* | | | | | | | | | | | | | |
| Rastenberger granodiorite | | 328±4 | | | | *F97* | | | | | | | | | | | | | |
| Rastenberger granodiorite | 623; >1206 | 338±2 | | | | *KP96* | | | | | 334±7 (amph, fsp,wr) | | *V92* | | | | | | |
| Rastenberger granodiorite | | 323±3 | | | | *Fr93* | | | | | | | | | | | | | |
| Freistadt granodiorite | | | 302±2 | | | *Fr92* | | | | | | | | | | | | | |
| *Oberpfalz* | | | | | | | | | | | | | | | | | | | |
| "Redwitzites" (diorites) | | 323±4 | | 322±4 | | *S03* | | | | | | | | | | | | | |
| Leuchtenberg granite | | 342±6 | | | | *KH96* | 325±4 | *S03* | | | 324±9 (wr, pl, kfs, bt) | 0.7078±1 | *KM76* | 323.9±0.5 | | | S95a | | |
| | | | | | | | | | | | 326±2 | | *S95a* | | | | | | |

| | | | | | | | | | | | | | | | | | |
|---|---|---|---|---|---|---|---|---|---|---|---|---|---|---|---|---|---|
| Zainhammer granite | | | | | | 321±1 | *S03* | 313.8±2.3 | | | | *W88* | 308.4±0.6 | | *W88* | 317–305 (ms,bt) | W92 |
| Falkenberg granite | | 307±22 | | 307±22 (wr,min) | *Ca89* | 315±4 | *S03* | 307±1 | 301±1 | 311±4 | 0.7097±8 | *W86* | 309.8±0.6 | 300±1 | *W86* | 303±1 (bt) | W92 |
| Liebenstein granite | | | | | | 315±2 | *S03* | 300<br>314 | | 320±40 | 0.7108±37 | *W86*<br>*W86* | | | | | |
| Mitterteich granite | | | | | | 310±7 | *S03* | | | 310±3 | 0.7104±5 | *S95b* | 310.3±0.5 | | *S95b* | | |
| Flössenburg granite | | | | | | 310±3 | *S03* | | | 312±3 | 0.7144±17 | *W94* | 299.6±0.5 | | *W94* | 301±1 (ms) | *W94* |
| | | | | | | | | | 293±5 (wr,pl, kfs) | | *W94* | | | | | | |
| Bärnau granite | | | | | | | | | | 313±2 | 0.7151±23 | *W94* | 305±0.6 | | *W94* | 308±1 (ms) | *W94* |
| Kreuzstein granite | | | | | | | | | | 297±2 | 0.737±28 | *BS95* | 303.1±0.9 | | *BS95* | | |
| Friedenfels granite | | | | | | 312±4 | *S03* | 309.2±1.5 | W88 | 315±2 | 0.7076±11 | *W92* | 308.1±0.4 | | *W88* | | |
| Steinwald granite | | | | | | 311±3 | *S03* | 306.1±5.6 | W88 | 310±1 | 0.7188±15 | *W92* | 306.5±0.4 | | *W88* | | |
| Neunburg granite | | 319.2±3.6 | | | *Ch03* | | | 310±6 | A73 | | | | 324±6 | 323±5 | *H67, Kreu89* | | |
| Oberviechthal granite | ~320 (Pb-loss) | | | | *Ch03* | | | | | | | | | | | | |

Note that HT/LP metamorphism and post-collisional magmatism are almost contemporaneous, ages become younger from Austria towards the Oberpfalz. Older intrusions also show geochemical differences in most cases (i.e. more basic, I-type or I/S-type, e.g. Finger et al., 1997; Siebel et al., 1997, 2003). References: A73 = Ackermann (1973), Br95 = Brandmayr et al. (1995), BS95 = Breiter and Siebel (1995), C91 = Christinas et al. (1991a), C91 = Christinas et al. (1991b), Ca89 = Carl et al. (1989), Ch03 = Chen et al. (2003), Ch04 = Chen and Siebel (2004), DS62 = Davis and Schreyer (1962), FF91 = Frasl and Finger (1991), FQ92 = Finger and von Quadt (1992), Fr92 = Friedl et al. (1992), Fr93 = Friedl et al. (1993), Fr96 = Friedl et al. (1996), Fr97 = Friedl (1997), G74 = Grauert et al. (1974), G89 = Gebauer et al. (1989), H67 = Harre et al. (1967), Horn86 = Horn et al. (1986), K89 = Köhler et al. (1989), Ka00 = Kalt et al. (2000), KH96 = Köhler and Hölzl (1996), Kl01 = Klötzli et al. (2001), KM76 = Köhler and Müller-Sohnius (1976), KM85 = Köhler and Müller-Sohnius (1985), KM86 = Köhler and Müller-Sohnius (1986), KP96 = Klötzli and Parrish (1996), Kreuz89 = Kreuzer et al. (1989), P00 = Propach et al. (2000), P91 = Propach et al. (1991), QF91 = von Quadt and Finger (1991), Sc87 = Scharbert (1987), S95a = Siebel (1995a), S95b = Siebel (1995b), S03 = Siebel et al. (2003), S05 = Siebel et al. (1995), S06 = Siebel et al. (2006), SS84 = Schulz-Schmalschäger et al. (1984), T04 = Teipel et al. (2004), V92 = Vellmer (1992), W86 = Wendt et al. (1986), W88 = Wendt et al. (1988), W92 = Wendt et al. (1992), W94 = Wendt et al. (1994).

mineral abbreviations after Kretz (1983).

LCI, UCI: Lower, upper concordia intercept.

wr: hole rock.

*Pb–Pb data are supported by additional U–Pb data.

and 312 Ma (Davis and Schreyer, 1962; Harre et al., 1967; Christinas et al., 1991b; Fig. 11, Table 4). A mantle component is present within the late porphyritic dacite dykes, which yielded a Rb–Sr whole rock-apatite-biotite isochron age of 302±7 Ma for the Kirchstein quarry. Due to the small thickness of the examined dyke, the age has been interpreted as intrusion age (Christinas et al., 1991b). A similar age of 299± 2.3 Ma (Propach et al., in press) was obtained by U–Pb dating of zircon for a dyke near Oberfrauenberg.

The cooling ages agree well with cooling ages of the adjacent Sauwald zone, the latter indicating temperatures of ca. 300 °C at about 300 Ma (Scharbert et al., 1997; Tropper et al., 2006). Thus cooling was protracted in the Passauer Wald and the Sauwald zone in comparison with other areas of the Bohemian Massif (see also Scharbert et al., 1997).

### *5.3. Implications of emplacement level on metamorphism and cooling of the Passauer Wald region*

The emplacement pressure of the Hauzenberg pluton is regarded as a minimum value for the high-temperature metamorphism and anatexis of the country rock, since regional metamorphism clearly pre-dates the intrusion. Apart from the phengite-barometric data, which are similar to those determined by Massonne (1984), the emplacement depth of the Hauzenberg pluton is further constrained by the growth of andalusite that is present within both the Hauzenberg granite I and the Hauzenberg granite II (Dollinger, 1967). Published Pressure estimates for the $Al_2SiO_5$ triple point are ranging from ca. 6 to 3.5 kbar (e.g. Richardson et al., 1969; Pattison, 1992; Holdaway and Mukhopadhay, 1993). Despite this uncertainty, the emplacement pressure determined for the Hauzenberg granite II (4.6±0.6 kbar) should be close to this triple point, i.e. growth of andalusite was just possible at mid crustal levels (16–18 km) (c.f. Clarke et al., 2005). As the Saldenburg granite (315± 3 Ma; Chen and Siebel, 2004) is younger than the Hauzenberg granite II but has a similar emplacement depth (see above), significant exhumation between 320 and 315 Ma can be ruled out. The additional data from the Taxberg granitic dyke also indicate that the main magmatic phase was not accompanied by decompression in the eastern Bavarian Forest.

The intrusion depth of the Rastenberg granodiorite in Austria (ca. 9–10 km, Büttner and Kruhl, 1997) is much lower than the 16–18 km determined for the Hauzenberg pluton. The age of the Rastenberg pluton, however, might be very similar to emplacement age of the Hauzenberg granite (Table 4, Fig. 11). On the other hand the Austrian Eisgarn granite (S-type leucogranite) might have an emplacement level similar to the Hauzenberg granite, as indicated by primary muscovite and andalusite (Vellmer and Wedepohl, 1994), but is older. Two-mica granites in the Czech Republic, such as the Lásenice granite (Breiter and Koller, 1999) and granites from the Ševéntin Massif (Matějka et al., 2003) also should have crystallized at pressures >3 kbar. The Weinsberg granites and most Bavarian granites should have lower emplacement levels than the Hauzenberg granite, as primary muscovite is absent within these rocks.

Unfortunately, there is no robust age of high-temperature metamorphism of the country rock for the Passauer Wald. This information is crucial to understand the linkage between magmatism and metamorphism. Based on results obtained elsewhere in the Bavarian Forest a gap of 2–6 m.y. between HT-metamorphism and magmatism is considered (Fig. 10). In the Bodenmais area (northern Bavarian Forest) the age of HT metamorphism is well constrained at 321–326 Ma (U–Pb on zircon, monazite and titanite; Kalt et al., 2000). Zircons and monazites separated from the Oedwies granodiorite yielded lower concordia intercepts at 326±5 and 329±9 Ma (Propach et al., 2000). U–Pb SHRIMP analyses of metamorphic overgrowths on Cadomian magmatic zircons from metagranitoids and metabasites of the Passau area yielded 319±5 Ma, 316±10 Ma (pooled mean age of recrystallized rims interpreted as metamorphic zircon growth), and 313± 5 Ma (single rim age interpreted to reflect a metamorphic overprint), respectively (Teipel et al., 2004). According to the author the nature of examined zircon rims is rather complex and the size of the individual growth zones is below SHRIMP resolution. The rims formed multi-temporally by both metamorphism and hydrothermal fluid-rock interaction. Compared with the new magmatic ages of the Hauzenberg pluton the aforementioned ages cannot reflect the metamorphic peak, but could indicate the retention of higher temperatures (amphibolite facies) along major shear zones. Rocks of the adjacent Sauwald zone yielded monazite ages that cluster around 321 Ma (microprobe dating; Tropper et al., 2006) and 316 Ma (U–Pb TIMS dating; Gerdes et al., 2006).

Considering the aforementioned age-data, high-temperature metamorphism and anatexis in the Hauzenberg area should have ceased only a few million years before the Hauzenberg granite intruded.

Despite a relatively short period between regional metamorphism and intrusion, contacts of the Hauzenberg pluton are discordant and sharp. The lack of re-

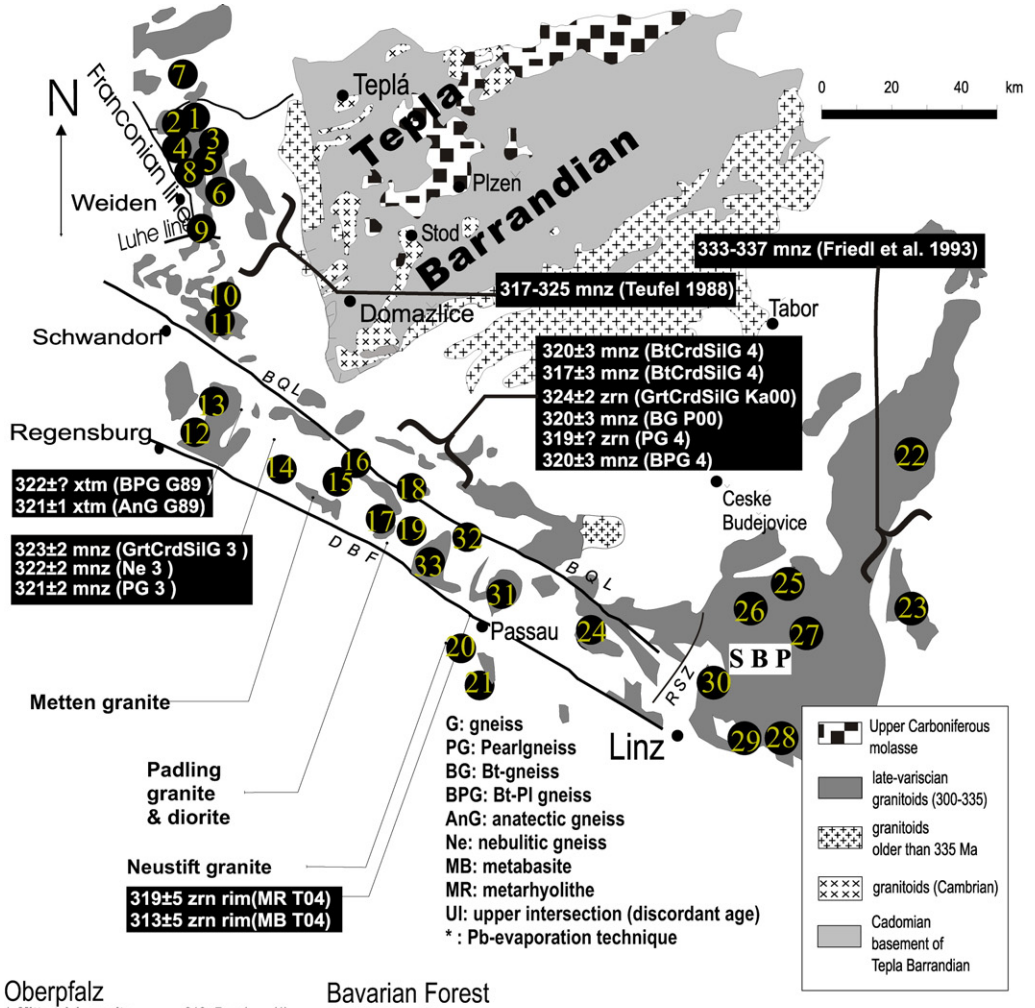


## Oberpfalz

| | | |
|---|---|---|
| 1: **Mitterteich granite:** | 310±7 zrn* | (1) |
| **2: Friedenfels granite:** | 312±4 zrn* | (1) |
| **3: Falkenberg granite:** | 315±4 zrn* | (1) |
| **4: Zainhammer granite:** | 321.1±1.2 zrn* | (1) |
| **5: Liebenstein granite:** | 315±2 zrn* | (1) |
| **6: Flössenburg granite:** | 310±3 zrn* | (1) |
| **7: Marktredwitz granite:** | 324±4(?)zrn* | (1) |
| **8: "Redwitzites"** | 323±4 zrn | (1) |
| | 322±4 ttn | (1) |
| **9: Leuchtenberg granite** | | |
| | 342 ±6 zrn-UI (KH96) | |
| | 321-329 zrn* | (1) |
| **10: Oberviechtach granite:** | ~ 320 zrn | (2) |
| **11: Neunburg granite:** | 322 ±4 zrn | (2) |

## Bavarian Forest

| | | |
|---|---|---|
| **12: Kristallgranit 1** | | |
| Kfs-porhyric granite: | 315±4 zrn | (3) |
| **13: Trasching granite:** | 321±3 mnz | (3) |
| **14: Oedwies granodiorite:** | 319±3 zrn | (3) |
| **15: Patersdorf granodiorite:** | 319-326 zrn* | (5) |
| | 325±3 zrn | (S06) |
| **16: Kollnburg granodiorite:** | 322 zrn | (4) |
| **17: Qtz-mica diorite:** | 310±? zrn | (4) |
| **18: Rinchnach granite:** | 317-331 zrn* | (5) |
| **19: Saunstein granodiorite** | | |
| | 325-342 zrn | (S05b) |
| **20: Platte granite:** | 311±2 mnz | (3) |
| **21: Schärding granite:** | 319±6 mnz | (8,7) |
| **31: Hauzenberg granite II:** | 320±3 zrn | (this study) |
| **Hauzenberg granodiorite:** | 318.6±4 zrn* | (this study) |
| **32: "Palite" (Frentzel 1911):** | | |
| metadiorite: | 334±3 zrn | (S05a) |
| **33: Fürstenstein complex:** | | |
| Diorites | 334±1 zrn* | (9) |
| Tittling granite | 323±1 zrn* | (9) |
| Eberhardsreuth granite: | 314±2 zrn* | (9) |
| Saldenburg granite | 315±3 zrn* | (9) |

## Austrian Moldanubian

| | | |
|---|---|---|
| **22: Eisgarn granite:** | 327±4 mnz | (8;7) |
| **23: Rastenberg Pluton:** | 338±2 zrn | (KP96) |
| | 328±4 zrn | (7) |
| | 323±3 zrn | (Fr93) |
| **24: Weinsberg granite** (Sarleinsbach complex): | 345±5(?)zrn* | (Kl01) |
| **25: Weinsberg granite** (Altweitra): | 328±5 mnz | (6) |
| **26: Weinsberg granite** (Plochwald): | 318±4 mnz | (QF91) |
| **27: Weinsberg granite** (Langschlag): | 323±4 mnz | (6) |
| **28: Weinsberg granite** (Grein): | 327±5 mnz | (6) |
| **29: Weinsberg granite** (Naarntal): | 327±5 mnz | (6) |
| **30: Freistadt granodiorite** | 302±2 mnz | (Fr92) |

Fig. 10. Regional distribution of U–Pb and Pb–Pb ages of zircon and monazite. Inverse labels indicate ages of HT-metamorphism. Most ages are concordant. Ages are given in Ma. Mineral abbreviations after Kretz (1983). References: 1 = Siebel et al., 2003, 2 = Chen et al., 2003, 3 = Propach et al., 2000, 4 = Grauert et al., 1974, 5 = Siebel et al., 2006, 6 = Friedl et al., 1996, 7 = Friedl, 1997, 8 = Frasl and Finger, 1991, 9 = Chen and Siebel, 2004, for other short references (G89, T04, Ka00, etc.) see Table 4. BQL = Bavarian Lode shear zone; DBF = Danubian fault; RSZ = Rodl shear zone.

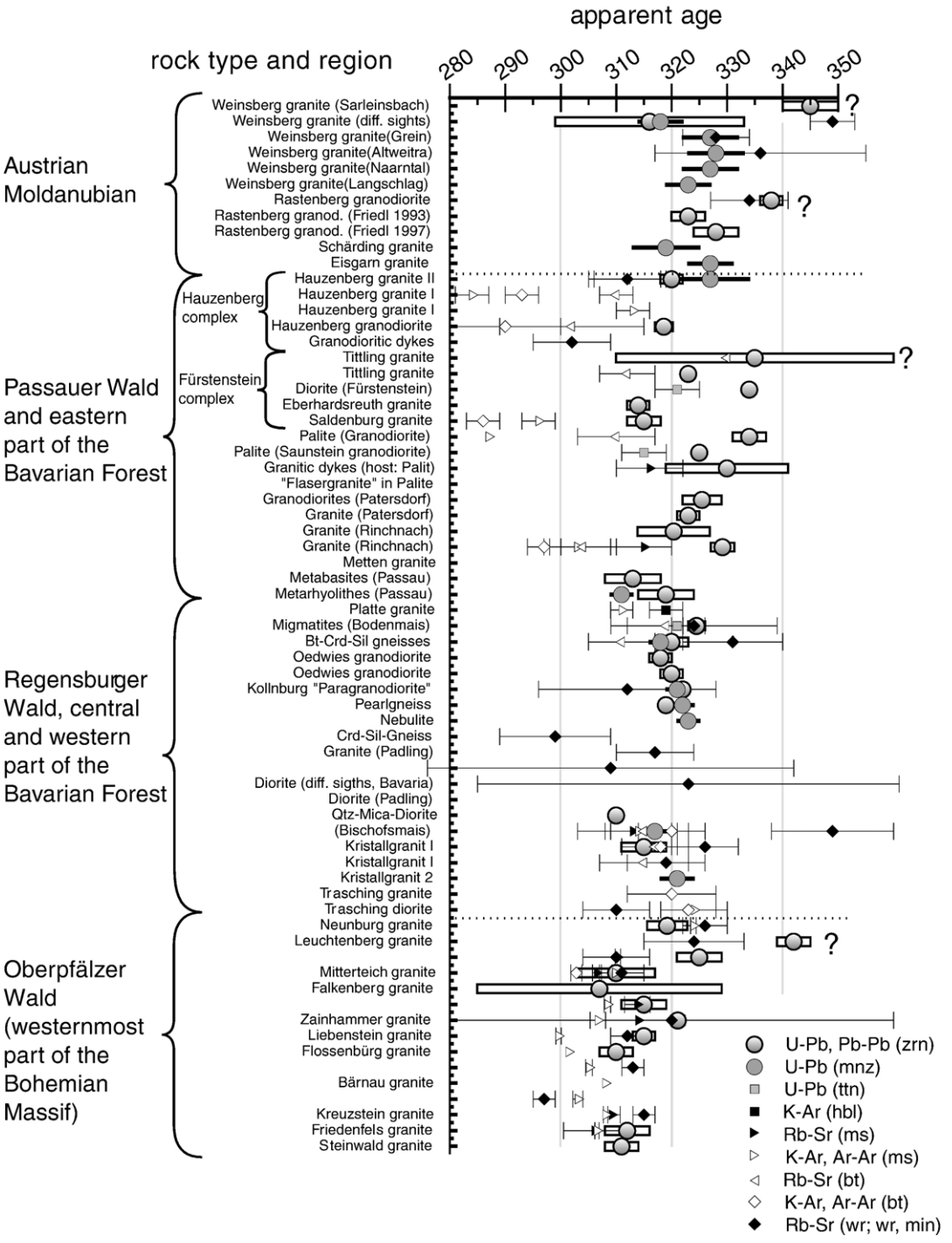


Fig. 11. Graphical illustration of ages derived from different isotopic systems. Mineral abbreviations after Kretz (1983), wr = whole rock isochron, min = mineral isochron. Error of U–Pb zrn = white box, U–Pb mnz = black bar, errors of other age-dating techniques = crosswing. Note that cooling ages from the Passauer Wald show a relatively wide scatter when compared with those from the central or western part of the Bavarian Forest. U–Pb and Pb–Pb ages become younger systematically from the Austrian Moldanubian towards the Oberpfalz. Especially ages older than 330 Ma have been doubted or discussed controversially either by the authors themselves (Davis and Schreyer, 1962; Tittlinger granite) or by others (Rastenberg pluton, Leuchtenberg granite, Weinsberg granite at Sarleinsbach). Such ages are marked with a question-mark. Further details are given in text.

melting and assimilation of xenoliths, as well as the coexistence of andalusite and sillimanite in rocks very close (<0.5 km) to the pluton suggest the country rock to have cooled to temperatures of 550–650 °C prior to the emplacement of the Hauzenberg granites I and II (Berger et al., 2002). *P–T* estimates for the HT-metamorphism of the country rock yield ca. 800 °C and 4–7 kbar (Klein, unpubl. data). Within the Sauwald zone *P–T* estimates show rather similar temperatures, but lower pressures (800 °C and 3–5 kbar; Tropper et al., 2006). Tropper et al. (2006) furthermore recognized discrepancies with earlier thermobarometric studies, which could mean that numerous *P–T* estimates, which have been carried out within the Bavarian Moldanubian in the last century, are too low.

If the age of metamorphism in the Passauer Wald does not differ significantly from that of the northern Bavarian Forest, cooling of ca. 200 °C was rapid and therefore requires exhumation. A cooling rate of ca. 100 °C/Ma for ca. 2–3 Ma just after peak-metamorphism, as it has been reported by Kalt et al. (2000; Bodenmais area), could apply to the Passauer Wald as well. Considering a geothermic gradient of 30 °C/km or higher, magma generation took place at <26 km depth, based on the calculated melt temperature of 780 °C. The emplacement of the granites occurred at ca. 16 km, suggesting a geothermic gradient of ca. 40 °C/km at 320 Ma. If melt building, metamorphism and prograde anatexis should have been approximately coeval, the absolute amount of elevation during and after anatexis was ca. 10 km or less. Therefore it would hardly be recognized by thermobarometric investigations.

### 5.4. Emplacement ages obtained off-site the Bavarian Forest

Within the Austrian–Czech Moldanubian most granitoids are part of the South Bohemian Pluton. Individual magma bodies have been subdivided taking into account compositional, petrographic and geochemical characteristics as well as intrusion ages (Weinsberg, Rastenberg, Eisgarn, Mauthausen Group) (Frasl and Finger, 1991; Vellmer and Wedepohl, 1994; Gerdes, 1997). According to Gerdes et al. (2003) about 80% of the South Bohemian Batholith formed between 331 and 323 Ma.

The Weinsberg granites in Austria (mainly syntectonic, coarse grained granites with K-feldspar megacrysts) show slightly older U–Pb ages than the Hauzenberg granitoids (von Quadt and Finger, 1991; Friedl et al., 1996; Gerdes et al., 2003). Zircon ages of ~350 Ma have been obtained by Klötzli et al. (2001) for specific granitoids of the Weinsberg type (Sarleinsbach quartz-monzodiorite), contradicting the results of other works (Finger and Clemens, 1995; Büttner and Kruhl, 1997; Gerdes et al., 2003), where the main intrusion phase of the Weinsberg granites occurred at ~328 Ma (Finger and Clemens, 2002; Klötzli et al., 2002; Gerdes et al., 2003).

With a U–Pb single-grain monazite age of 316±1 Ma (Gerdes et al., 2003) the I-type Mauthausen granite could be an analogue to the Hauzenberg granodiorite, although the former contains some muscovite. The Mauthausen Group encompasses fine- to medium-grained posttectonic granites and granodiorites (Vellmer and Wedepohl, 1994; Gerdes, 1997).

The Rastenberg granodiorite of the South Bohemian Pluton (Lower Austria) has been dated at 323±2 Ma and 328±4 Ma (Friedl et al., 1993; Friedl, 1997). However, Klötzli and Parrish (1996) obtained a rather different U–Pb age for this rock of 338±2 Ma using short-prismatic zircons. A possible explanation for contrasting isotopic age data is that the Rastenberg pluton is not built up by a homogenous magma (see also Gerdes et al., 2000b). Comparable ages were reported for the Leuchtenberg granite of the Bavarian Oberpfalz (342±6 Ma upper intercept age, U–Pb on zircon, Köhler and Hölzl, 1996). However, the quality of this age has been doubted by Siebel et al. (2003) concerning metamictization (see also Grauert et al., 1996). Siebel et al. (2003) propose a significantly younger Pb–Pb zircon-evaporation age of 325±4 Ma which matches ages of adjacent granites, all of which are younger than 320 Ma (Figs. 10 and 11, Table 4, Siebel et al., 2003). The Redwitzite suite of NE Bavaria yielded Pb–Pb ages between 325 and 320 Ma, consistent with U–Pb titanite ages (Siebel et al., 2003). Field relations indicate the Redwitzites (diorites) to be older than the Leuchtenberg granite (René, pers. comm.). Thus the main emplacement of the Leuchtenberg granite should be younger than 325 Ma.

### 5.5. Ages of metamorphism and cooling in other parts of the Bohemian Massif

Rapid cooling is typical for Moldanubian rocks of the Bohemian Massif (Fritz and Neubauer, 1993; Petrakakis, 1997; Fig. 11). The timing of HT/LP metamorphism of Moldanubian rocks from the Oberpfalz has been dated at 317–325 Ma (concordant U–Pb monazite ages by Teufel, 1988). Here the ages of metamorphism, plutonism and cooling already stress the resolution of geochronology (Table 4, Fig. 11).

The age of metamorphism in the North-Austrian Monotonous group is constrained at 333–337 Ma

(concordant monazite ages, Friedl et al., 1993; Gerdes et al., 2006). The Variegated Series (Dobra gneiss at its base) yields metamorphic ages of 333±2 and 336±3 Ma (Friedl et al., 1994; Gebauer and Friedl, 1994;). $^{39}Ar$–$^{40}Ar$ hornblende cooling ages indicate rapid cooling below ca. 500 °C for the Variegated group (328.7±1.3 and 341.1±1.4 Ma, respectively; Dallmeyer et al., 1992). Diffusion modeling of garnet indicates fast cooling (100–165 °C) and exhumation rates exceeding 7 mm/a for eclogites associated with the HP-metamorphic Gföhl Unit (Medaris et al., 2006).

Ar–Ar cooling ages of rocks from the central Bohemian Massif tend to become younger towards south, yielding approximately 320 Ma in the area of Gmünd and ca. 290 Ma in the block located south of the Bavarian and the Bohemian Lode (Scharbert et al., 1997).

Rapid uplift and associated cooling is also documented at the northern margin of the Bohemian Massif within the Saxothuringian belt at the Krusné Hory/Erzgebirge (e.g. Konopaśek and Schulmann, 2005).

### 5.6. Geodynamic model

Although more metamorphic and magmatic ages from the Moldanubian unit would be desirable (especially from the area north of the Bavarian Pfahl), HT-metamorphism, anatexis and magmatism are obviously related processes.

Relying upon existing age data (Table 4), it is believed that the generation of melt and HT-metamorphism took place simultaneously at a regional scale in response to partial delamination of the lithospheric mantle. Before decompression induced large-scale melting, the crust was already pre-heated by radiogenic heat and possibly first melts have been formed as well. After partial mantle delamination exhumation of ca. 3–10 km (compare Henk et al., 2000) led to dehydration melting of muscovite and biotite resulting in additional melt. This scenario would be consistent with qualitative *P–T* paths of Kalt et al. (1999), which indicate melt formation at pressures of ca. 5–7 kbar and crystallization below 5 kbar. The *P–T-t* cooling-path of Kalt et al. (2000) also starts at slightly elevated pressures of 5–7 kbar. Finally, as decompression ceased the emplacement of numerous plutons occurred contemporaneously in mid- to high crustal levels. Subsequent cooling of the crust was afterwards related to local tectonics, the latter resulting in differential uplift and exhumation. K–Ar and Rb–Sr cooling ages of the Hauzenberg granitoids (Harre et al., 1967) are indicative for sustained exhumation or the successive retreat of anomalously lifted isotherms within the following 10 m.y. after melt emplacement. Based on slightly younger ages (Chen and Siebel, 2004) but similar emplacement depths (Massonne, 1984; Dietl et al., 2005) of the adjacent Saldenburg granite, the latter is probable. The Hauzenberg area cooled more protracted than rocks from the northwestern Bavarian Forest and the Oberpfalz (Table 4, Fig. 11). This difference can be explained by a higher crustal thickness in the Passauer Wald, as already supposed by Olbrich (1985). For many other Moldanubian plutons the gaps between crystallization and cooling ages are tight (Fig. 11, Table 4). In all these cases HT-metamorphism, uplift and even cooling must have had the character of a significant geological event.

Exact age-dating of HT-metamorphism could lead to a substantial refinement of this view, particularly if new data would point to a larger time gap between HT-metamorphism and magmatism or to the existence of an older, second anatexis (see also Tropper et al., 2006; Gerdes et al., 2006; Finger and Gerdes, 2006). In case of the Oberpfalz the gap between plutonism and magmatism appears to be larger than in other regions (Teufel, 1988). However, S-type magmatism appears to be delayed in comparison with the Bavarian Forest.

### 5.7. Synthesis

The age of 320±3 Ma reported for the Hauzenberg granite II as well as the age of 318.6±4.1 Ma for the Hauzenberg granodiorite are consistent with published cooling ages. They furthermore agree with ages, which have been reported from adjacent granitoids including granites of the Weinsberg and Mauthausen type (Table 4). A correlation of the easternmost Bavarian granites with Weinsberg granites from the South Bohemian Pluton appears likely based on intrusion ages, but only a distinct geochemical investigation would clarify if a genetic relation exists. Affinity with the Eisgarn type is ruled out by a much lower initial Sr-ratio of the Hauzenberg granite II that points to a magma generation at deeper crustal levels (0.7089±1; Christinas et al., 1991b). The two-mica granites of the ševetin Massif and the Hauzenberg granite I show some petrographic similarities such as biotite aggregates and large rounded cordierite grains, but the melt temperatures of the former are quite low (ca. 700 °C, Matějka et al., 2003).

The Hauzenberg granodiorite could represent an equivalent to older granites belonging to the Mauthausen Group.

As major structural elements are missing between the Regensburger and the Passauer Wald, metamorphism is

likely coeval for both regions and in consequence only few m.y. older than the intrusion ages determined here. Generation of the Hauzenberg melt and anatexis are approximately coeval but the generation of larger melt volumes took place at slightly deeper structural levels at granulite facies conditions. Since anatectic features can be spotted almost everywhere in the Bavarian Forest, they are interpreted to result from decompression. Large-scale melting started during upper amphibolite to granulite facies metamorphism, as indicated by the complete lack of muscovite and features of biotite breakdown within anatectic gneisses at pressures >5 kbar (Kalt et al., 1999, 2000). Relics of hypersthene, garnet and hercynite, which are occurring in different migmatites as well as pseudomorphs of sillimanite after kyanite in granulites south of the Hauzenberg pluton (Felber, 1987), could allow to narrow down the pressure limits during late-Variscan metamorphism and related anatexis, as long as mineral growth can be assigned to Carboniferous metamorphism. It has to be emphasized that relics of medium pressure metamorphism of unknown age are by far not restricted to the Passauer Wald (O'Brien, 2000 and references therein).

For the Moldanubian region several origins of HT/LP-metamorphism and LP anatexis were debated. Among them (a) emplacement of hot granulites, (b) advective heat transfer by wide-spread magmatism, (c) radiogenic heat transfer or (d) removal of the thermal boundary layer or the lithospheric mantle (Henk et al., 2000 and references therein). In contrast to O'Brien (2000), the emplacement of hot granulitic slices in the mid-crust as a melt generating process is not considered here. Their low overall volume within the Bavarian Moldanubian and their minor heat-capacity would allow anatexis in direct contact to granulite facies rocks, but large-scale melting is unlikely, considering that melting itself consumes heat. Advective heat transfer by granitic magma provided heat to sustain elevated temperatures, but anatexis of metabasites as occurring within the Passauer Wald requires temperatures higher than typical melt temperatures of granite. The emplacement of larger magma bodies also seems to post-date the major anatexis. Additionally it is even doubtful whether advective heat transfer in the form of granitic magmatism can cause wide-spread anatexis at low pressures, especially if magmatic flow is non-pervasive (Gerbi et al., 2006). Radiogenic heat on the other hand can cause anatexis (Gerdes et al., 2000a), but would lead to isobaric heating. Heat production would cease as soon as melts form and escape, thereby disturbing the heat-producing layer. Thus melting of amphibolites is unlikely to be induced by this process as well. Another problem with radiogenic heat is that the relatively short time-frame requires a very similar nature (thickness, abundance of radiogenic elements and time of formation) of the heat-producing layer throughout the entire Moldanubian zone. Following Arnold et al. (2001), Gerbi et al. (2006) doubt radiogenic heat to be a primary source of LP anatexis: high heat production may cause melting at low pressure, but the temperatures below the Upper Crust would reach extreme values well above 1000 °C. The same holds true for a complete delamination of the mantle lithosphere.

One of the key results of Gerbi et al. (2006) is that the aforementioned processes (b–d) in addition to crustal thinning are unlikely to cause LP anatexis if they operate exclusively, whereas a combination of them is not. On the other hand numerous world-wide examples (e.g. Whitney et al., 2003) demonstrate that (near)-isothermal decompressional melting probably is a more viable mechanism to melt down large volumes of rock.

Existing U–Pb and Pb–Pb data of Moldanubian granitoids and high-grade metamorphic rocks suggest that late- to post-kinematic magmatism and HT/LP metamorphism occurred delayed towards the northwest in the western part of the Bohemian Massif (Figs. 10 and 11). Both processes started at ca. 325–340 Ma within the Austrian Moldanubian unit and migrated northwestward or westward. A temporal change of magmatism from NE to SW cannot be recognized yet as magmatic age data from the area situated north of the Bavarian Lode shear zone are lacking (Fig. 11) and the absolute displacement along this dextral fault zone is unknown. Based on several new U–Pb TIMS age data of monazite, which cover anatectic rocks from the Böhmerwald (ca. 335 Ma) and from the Austro-Bavarian Moldanubian (Muehl and Sauwald zone; 314–326 Ma to the north and 314–317 Ma to the south of the Danubian fault, respectively), Gerdes et al. (2006) proposed a southwestward progression of the late-Variscan heat front. However, age-shifting within the underlying dataset could partially result from dextral displacements along the Bavarian Lode shear zone and the Danubian fault, respectively. Gerdes et al. (2006) also recognized inherited monazite components with inferred ages of ca. 335–340 Ma pointing to earlier metamorphism (possibly earlier anatexis as well?).

Mineral cooling ages from the easternmost Moldanubian unit indicate subsequent cooling below 500 °C at 325–343 Ma ($^{39}$Ar–$^{40}$Ar on hornblende, Dallmeyer et al., 1992). Within the South Bohemian Pluton the major magmatic events and metamorphism took place ~7 Ma earlier as in the Bavarian Forest. Within the Northern Oberpfälzer Wald, where radiometric data are

extraordinarily consistent, magmatism occurred 5–7 Ma later than in the Bavarian Forest. Exceptions are the Leuchtenberg granite and the redwitzites (dioritic to tonalitic crustal rocks with mantle components), both of which differ in their geochemical composition from the adjacent S-type granites (Siebel et al., 1997). The redwitzites (dioritic to tonalitic magmatites) can be treated as equivalents to durbachites (coarse-grained, High-K, Mg melagranite-melasyenite porphyries; Holub et al., 1997), which occur within the Austrian-Czech part of Moldanubian as well as in the Black Forest and the Vosges (Siebel et al., 1999). Redwitzites and durbachites both contain material derived from an enriched lithospheric mantle (Finger et al., 1997; Gerdes, 1997; Siebel et al., 1997) and their formation must be related to changes (e.g. decompression by isostasy, heating) affecting the latter. Recently, enriched gabbros were spotted in contact with the Jihlava and the Trébič durbachite. This observation by Leichmann et al. (2003) not only gives direct evidence that durbachites originated as magma mixtures of partially molten crustal rocks and mantle melts, but further indicates that mixing took place at the present outcrop-level of the Central Bohemian Pluton.

However, significantly younger redwitzite ages reported by Siebel et al. (2003) question a close relationship between redwitzites and durbachites, since durbachitic magmatism is supposed to have had an event-like character at about 340 Ma (Schaltegger, 1997; Kotkova et al., 2003; Janoušek and Gerdes, 2003; Verner et al., 2006). On the other hand recent age dating of durbachites located in the eastern Bohemian Massif yielded ages, which are substantially younger than 340 Ma (ca. 323 Ma, Schulmann et al., 2005).

Granite emplacement ages from the Southern Oberpfälzer Wald were reported by Chen et al. (2003): these granites are geochemically and geochronologically closer related to those of the Bavarian Forest and moreover gave similar ages of ~320 Ma. Their geochemical signature suggests that melting took place under granulite facies conditions (Chen et al., 2003).

As a cause for the temporal shift of metamorphism and related magmatism removal of either the lithospheric mantle (partial delamination) or the thermal boundary layer of the thickened Variscan crust, as suggested by Zulauf (1997), Henk et al. (2000) and Arnold et al. (2001), appear most likely. Older and more basic intrusives such as the redwitzites (diorites to tonalites), the durbachites (melagranites–syenites) or even the diorites of the Bavarian Forest (including the palites) could represent melts that directly resulted from partial delamination. Within the Moldanubian of the Bohemian Massif this removal might have advanced at high angle to the major zone boundaries starting in today's southeastern part of the Bohemian Massif and moving subsequently northwestward towards the Saxo-Thuringian. The immediate consequence of mantle delamination is an overall density loss leading to buoyancy forces that trigger elevation, thus leading to raised topography and pronounced exhumation. Independent of how much lithospheric material is removed, the upwelling asthenosphere will cause intensive and fast heating, promoting the formation of melt (Zulauf, 1997; Arnold et al., 2001). The combination of upward movement of a crust, which already might have been in a thermally critical state due to intensive radiogenic heat production (internal heat source) with an external heat source at its bottom is the best explanation for the tremendous amount of melt generated within the Moldanubian area. During uplift syntectonic S-type granites, diatexites and "Schlieren granites" (Finger and Clemens, 1995) would form. Uplift would cease when the crust reaches isostatic equilibrium. The resulting stop of vertical movements leads to S-type magmatism of intrusive character. The contacts to anatectic rocks are often sharply discordant suggesting substantial cooling. An example is the contact of Weinsberg granites with diatexites as it has been described by Finger and Clemens (1995). Intrusive magmatism may also have triggered minor anatexis in the country rock in case of wet pelites, possibly associated with the formation of the non-deformed S-type granites, such as granites of the Eisgarn type or the "Schlierengranites" (Finger and Clemens, 1995). It follows a phase of more basic I/S-type magmatism, which might be related to either the successively increasing degree of partial melting or an enhanced crust/mantle interaction (Mauthausen-Freistadt suite). Post-orogenic granodiorite porphyries intruding into minor extensional shear zones might be explained by melting of hydrated lithospheric mantle (Gerdes, 1997; René, 1999).

An increased thickness of the lithospheric mantle in the area of the Southern Bohemian Pluton could be the reason, why delamination started there. A partial delamination appears more likely for the Moldanubian, since it would explain why most melts lack geochemical signatures of asthenospheric material — the role of the asthenosphere would then be reduced to provision of conductive heat (Zulauf, 1997). This scenario cannot be distinguished from a removal of the thermal boundary layer (Henk et al., 2000).

The systematic age-shift (Fig. 11) and similar radiogenic ages of neighbouring plutons as illustrated in Fig. 10 appear to be more compatible with a rapidly propagating process such as delamination rather than radiogenic heat production (e.g. Gerdes et al., 2000a;

O'Brien, 2000). The concurrence of metamorphism and magmatism combined with the observation that contacts between melts and migmatites are sharp, thus suggesting a relatively cold country rock, requires a heat-consuming process. The necessity for such a process rules out radiogenic heat as being the only cause involved. If continued radiogenic decay would be the only heat source, sharp intrusive contacts could not develop since magmatism and metamorphism would be completely coeval. Furthermore extensive exhumation should post-date anatexis and plutonism, otherwise the internal heat source would prolong.

Instead the wide dispersion of cooling ages in the Passauer Wald points to relatively slow exhumation rates after granite emplacement, although the intrusion of numerous intermediate dykes certainly contributed to sustain intermediate temperatures (~300 °C) throughout the Permian. The cooling path of the Passauer Wald region was probably comparable to rocks of the Austrian Sauwald zone (Tropper et al., 2006). Muscovite growth was dated by $^{40}Ar$–$^{39}Ar$ geochronology in the Austrian continuation of the Bavarian Lode shear zone. These micas indicate that elevated temperatures lasted to ca. 287 Ma inside mylonitic shear zones aligned parallel to the Bavarian Lode shear zone (Table 4; Brandmayr et al., 1995).

The combination of new and existing data allows the following conclusions to be drawn:

- the Variscan crust substantially cooled before the Hauzenberg pluton intruded at 320 Ma and probably was in isostatic equilibrium
- a deeper crustal level is exposed in the Passauer Wald than in other areas of the Bavarian Forest
- within the Passauer Wald late- to post-magmatic cooling was achieved by retrieval of anomalously raised isotherms rather than continuous exhumation
- in other regions of the southern Bohemian Massif the slightly different timing of magmatism and metamorphism suggests the heat source to have proceeded in a systematical manner, as to expect in course of a partial delamination of the lithospheric mantle

## Acknowledgements

We thank the Geological Survey at the Bavarian Environment Agency for financial support of field and laboratory work in the EFRE-Project "Schaffung geologischer und hydrogeologischer Informationsgrundlagen im Ziel 2-Gebiet". Christian Dekant is thanked for providing CL images of zircons from the Schachet granodiorite, which were photographed at the LMU in Munich. We furthermore acknowledge Ulrich Teipel for discussions. Careful and constructive revisions of the manuscript by Karel Breiter and Milos René are highly appreciated.

## References

Ackermann, W., 1973. Rb–Sr – Datierung einiger Gesteine des ostbayerischen Kristallins durch Gesamtgesteins – und Biotitanalysen. Geologica Bavarica 68, 155–162.

Arnold, J., Jacoby, B.R., Schmeling, H., Schott, B., 2001. Continental collision and the dynamic and thermal evolution of the Variscan orogenic crustal root — numerical models. Journal of Geodynamics 31, 273–291.

Behrmann, J.H., Tanner, D., 1997. Carboniferous tectonics of the Variscan basement collage in eastern Bavaria and western Bohemia. Geologische Rundschau 86 (Suppl.), S15–S27.

Benisek, A., Finger, F., 1993. Factors controlling the development of prism faces in granite zircons: a microprobe study. Contributions to Mineralogy and Petrology 114, 441–451.

Berger, F., Kiehm, S., Klein, T., Dörr, W., Zulauf, G., 2002. Alter und Intrusionstiefe des Hauzenberger Granits, Erlanger Geologische Abhandlungen. Sonderband 3, 9–10.

Brandmayr, M., Dallmeyer, R.D., Handler, R., Wallbrecher, E., 1995. Conjugate shear zones in the Southern Bohemian Massif (Austria): implications for Variscan and Alpine tectonothermal activity. Tectonophysics 248, 97–116.

Breiter, K., Koller, F., 1999. Two-mica granites in the central part of the South Bohemian pluton. Abhandlungen der Geologischen Bundesanstalt 56, 201–212.

Breiter, K., Siebel, W., 1995. Granitoids in the Rozvadov pluton. Geologische Rundschau 84, 506–519.

Büttner, S., Kruhl, J.H., 1997. The evolution of a late-Variscan high-T/low-P region: The southeastern margin of the Bohemian Massif. Geologische Rundschau 86 (1), 21–38.

Carl, C., Wendt, I., Wendt, J.I., 1989. U/Pb whole-rock mineral dating of the Falkenberg granite in northeast Bavaria. Earth and Planetary Science Letters 94, 236–244.

Chen, F.K., Siebel, W., 2004. Zircon and titanite geochronology of the Fürstenstein granite massif, Bavarian Forest, NW Bohemian Massif: pulses of the late Variscan magmatic activity. European Journal of Mineralogy 16 (5), 777–788.

Chen, F., Siebel, W., Satir, M., 2003. Geochemical and isotopic composition and inherited zircon ages as evidence for lower crustal origin of two Variscan S-type granites in the NW Bohemian massif. International Journal of Earth Sciences 92 (3), 172–184.

Cherniak, D.J., 1993. Lead diffusion in titanite and preliminary results on the effects of radiation damage on Pb transport. Chemical Geology 110, 177–194.

Cherniak, D.J., Watson, E.B., 2001. Pb diffusion in zircon. Chemical Geology 172 (1-2), 5–24.

Cherniak, D.J., Watson, E.B., 2004. Pb diffusion in monazite. Geochimica and Cosmochimica Acta 68 (4), 829–840.

Christinas, P., Köhler, H., Müller-Sohnius, D., 1991a. Altersstellung und Genese der Palite des Vorderen Bayerischen Waldes. Geologica Bavarica 96, 87–107.

Christinas, P., Köhler, H., Müller-Sohnius, D., 1991b. Rb–Sr Altersbestimmungen an Intrusiva des Hauzenberger Massivs, Nordostbayern. Geologica Bavarica 96, 109–118.

Clarke, D.B., Dorais, M., Barbarin, B., Barker, D., Cesare, B., Clarke, G., El Baghdadi, M., Erdmann, S., Förster, H.-J., Gaeta, M., Gottesmann, B., Jamieson, R.A., Kontak, D.J., Koller, F., Gomes,

C.L., London, D., Morgan VI, G.B., Neves, L.J.P.F., Pattison, D.R.M., Pereira, A.J.S.C., Pichavant, M., Rapela, C.W., Renno, A.D., Richards, S., Roberts, M., Rottura, A., Saavedra, J., Sial, A.N., Toselli, A.J., Ugidos, J.M., Uher, P., Villaseca, C., Visonà, D., Whitney, D.L., Williamson, B., Woodard, H.H., 2005. Occurrence and origin of andalusite in peraluminous felsic igneous rocks. Journal of Petrology 46 (3), 441–472.

Cloos, H., 1927. Plutone des Passauer Waldes. Borntraeger, Berlin. 182 pp.

Cocherie, A., Guerrot, C., Rossi, P., 1992. Single-zircon dating by step-wise Pb evaporation: comparison with other geochronological techniques applied to the Hercynian granites of Corsica, France. Chemical Geology 101, 131–141.

Dallmeyer, R.D., Neubauer, F., Höck, V., 1992. Chronology of Late Paleozoic tectonothermal activity in the Southeastern Bohemian Massif, Austria (Moldanubian and Moravo-Silesian Zones) — $^{40}Ar/^{39}Ar$ mineral age controls. Tectonophysics 210 (1–2), 135–153.

Davis, G.L., Schreyer, W., 1962. Altersbestimmungen an Gesteinen des ostbayerischen Grundgebirges und ihre geologische Deutung. Geologische Rundschau 52, 146–159.

Dietl, C., Göβmann, M., De Wall, H., 2005. Kombinierte aktive und passive Platznahme in einer verdickten Kruste — erste Ergebnisse von gesteinsmagnetischen und petrologischen Untersuchungen am Fürstensteiner Intrusivkomplex (Bayerischer Wald). Zeitschrift der Deutschen Geologischen Gesellschaft 155 (2–4), 311–328.

Dollinger, U., 1961. Geologisch Petrographische Untersuchungen im Südteil des Gradabteilungsblattes Waldkirchen. LM University Munich, pp. 1–63.

Dollinger, U., 1967. Das Hauzenberger Granitmassiv und seine Umrahmung. Geologica Bavarica 58, 145–172.

Dörr, W., Zulauf, G., Fiala, J., Franke, W., Vejnar, Z., 2002. Neoproterozoic to Early Cambrian history of an active plate margin in the Tepla-Barrandian unit — a correlation of U–Pb isotopic-dilution-TIMS ages (Bohemia, Czech Republic). Tectonophysics 352 (1–2), 65–85.

Felber, J., 1987. Geologische Studien in der Kropfmühl-Serie. Ph.D thesis, L.M.-University, Munich, 193 pp.

Finger, F., Clemens, J.D., 1995. Migmatization and "secondary" granitic magmas: effects of emplacement and crystallization of primary granitoids in South Bohemia, Austria. Contributions to Mineralogy and Petrology 120, 311–326.

Finger, F., Clemens, J.D., 2002. Cadomian lower-crustal contributions to Variscan petrogenesis (South Bohemian Batholith, Austria): a comment. Journal of Petrology 43, 1779–1781.

Finger, F., Gerdes, A., 2006. Neue Hypothesen zum Ablauf der variszischen Orogenese in der südlichen Böhmischen Masse: Durbachitische Intrusionen als Anzeiger für Slab break-off und die Bavarische Phase als Ausdruck spätvariszischer Delamination von Lithosphäre. Abstract volume Pangeo. Conference Series. Innsbruck University Press, Austria, pp. 57–58.

Finger, F., von Quadt, A., 1992. Wie alt ist der Weinsberger Granit? U/Pb versus Rb/Sr Geochronologie. Mitteilungen der Österreichischen Mineralogischen Gesellschaft 137, 83–87.

Finger, F., Roberts, M.P., Haunschmid, B., Schermaier, A., Steyrer, H.P., 1997. Variscan granitoids of central Europe: their typology, potential sources and tectonothermal relations. Mineralogy and Petrology 61 (1–4), 67–96.

Frasl, G., Finger, F., 1991. Geologisch-Petrographische Exkursion in den österreichischen Teil des Südböhmischen Batholiths. European Journal of Mineralogy 3 (2), 23–40.

Frentzel, A., 1911. Das Passauer Granitmassiv. Geognostisches Jahrbuch 24, 1–31.

Friedl, G., 1997. U/Pb-Datierungen an Zirkonen und Monaziten aus Gesteinen vom österreichischen Anteil der Böhmischen Masse. University of Salzburg, Salzburg, 242 pp.

Friedl, G., Frasl, G., von Quadt, A., Finger, F., 1992. Neue U/Pb Datierungen aus der südlichen Böhmischen Masse. Frankfurter Geowissenschaftliche Arbeiten A11, 217.

Friedl, G., von Quadt, A., Ochsner, A., Finger, F., 1993. Timing of the Variscan Orogeny in the Southern Bohemian Massif (NE-Austria) deduced from ne U–Pb zircon and monazite dating. EUG 5, Strassbourg, Terra Abstracts 5/1, 235–236.

Friedl, G., von Quadt, A., Finger, F., 1994. 340 Ma U/Pb-Alter aus dem österreichischen Moldanubikum und ihre geologische Bedeutung. Terra Nostra 3/94, 43–46.

Friedl, G., von Quadt, A., Finger, F., 1996. Timing der Intrusionstätigkeit im Südböhmischen Batholith. 6th TSK symposium, Salzburg, extended abstracts. Facultas-Universitätsverlag, Wien, pp. 127–130.

Fritz, H., Neubauer, F., 1993. Kinematics of crustal stacking and dispersion in the south-eastern Bohemian Massif. Geologische Runcschau 82, 556–565.

Galadí-Enríquez, E., Zulauf, G., Heidelbach, F., Rohrmüller, J., 2006. Insights into the post-emplacement history of the Saunstein granitic dyke showing heterogeneous deformation and inconsistent shear-sense indicators (Bavarian Forest, Germany). Journal of Structural Geology 28, 1536–1552.

Gebauer, D., Friedl, G., 1994. A 1.38 Ga protolith age for the Dobra orthogneiss (Moldanubian zone of the southern Bohemian Massif, NE Austria): evidence from ion-microprobe (SHRIMP) dating of zircon. Journal of the Czech Geological Society 39 (1), 34–35.

Gebauer, D., Williams, I.S., Compston, W., Grunenfelder, M., 1989. The development of the Central European continental-crust since the early Archean based on conventional and ion-microprobe dating of up to 3.84 B.Y. old detrital zircons. Tectonophysics 157 (1–3), 81–96.

Gerbi, C.C., Johnson, S.E., Koons, P.O., 2006. Controls on low-pressure anatexis. Journal of Metamorphic Geology 24, 107–118.

Gerdes, A., 1997. Geochemische und thermische Modelle zur Frage der spätorogenen Granitgenese am Beispiel des Südböhmischen Batholiths: Basaltisches Underplating oder Krustenstapelung?, Ph.D. thesis, Geochemisches Institut, Göttingen University, 113 pp.

Gerdes, A., Henk, A., Wörner, G., 2000a. Post-collisional granite generation and HT/LP metamorphism by radiogenic heating: the Variscan South Bohemian Batholith. Journal of the Geological Society of London 157, 577–587.

Gerdes, A., Wörner, G., Finger, F., 2000b. Hybrids, magma mixing and enriched mantle melts in post-collisional Varisian granotoids: the Rastenberg pluton, Austria. In: Franke, W., Haak, V., Oncken, O., Tanner, D. (Eds.), Orogenic Processes: Quantification and Modelling in the Variscan belt. London, Geological Society of London, vol. 179, pp. 415–432.

Gerdes, A., Friedl, G., Parrish, R.R., Finger, F., 2003. High-resolution geochronology of Variscan granites — the South Bohemian Batholith. Journal of the Czech Geological Society 48 (1–2), 70–71.

Gerdes, A., Finger, F., Parrish, R.R., 2006. Southwestward progression of a late-orogenic heat front in the Moldanubian zone of the Bohemian Massif and formation of the Austro-Bavarian anatexite belt. Geophysical Research Abstracts 8, 10698.

Grauert, B., Hänny, R., Soptrajanova, G., 1974. Geochronology of a polymetamorphic and anatectic gneiss region — Moldanubicum of area Lam-Deggendorf, Eastern Bavaria, Germany. Contributions to Mineralogy and Petrology 45 (1), 37–63.

Grauert, B., Abdullah, N., Glodny, J., Krohe, A., 1996. "Widersprüche" in der geochronologischen Information für Tiefbohrung

und Umfeld - Konsequenzen für die Aussagen zur tektonometamorphen Entwicklung der. 9th colloquium of the german continental Deep-Drilling Project (KTB), June, 20-21, 1996, Giessen, Germany.

Hanchar, J.M., Miller, C.F., 1993. Zircon zonation patterns as revealed by cathodoluminescence and backscattered electron images: implications for interpretation of complex crustal histories. Chemical Geology 110 (1–3), 1–13.

Harre, W., Kreuzer, H., Lenz, H., Müller, P., 1967. Zwischenbericht über K/Ar und Rb/Sr-Datierungen von Gesteinen aus dem ostbayerisch-österreichischen Kristallin. Bundesanstalt f. Bodenforschung, Datierungsbericht 5/67, Archiv-Nr. 25/338.

Henk, A., Blanckenburg, F., Finger, F., Schaltegger, U., Zulauf, G., 2000. Syn-convergent high temperature metamorphism and magmatism in the Variscides: a discussion of potential heat sources. In: Franke, W., Haak, V., Oncken, O., Tanner, D. (Eds.), Orogenic Processes: Quantification and Modelling in the Variscan belt. London, Geological Society of London, vol. 179, pp. 387–400.

Holdaway, M., Mukhopadhay, B., 1993. A reevaluation of the stability relations of andalusite: thermochemical data and phase diagram for the aluminium silicates. American Mineralogist 78, 298–315.

Holub, F., Cocherie, A., Rossi, P., 1997. Radiometric dating of granitic rocks from the central Bohemian Plutonic Complex (Czech republic): constraints on the chronology of thermal and tectonic events along the Moldanubian-Barrandian boundary. Comptes Rendus de l'Académie des Sciences Paris 325, 19–26.

Horn, P., Köhler, H., Müller-Sohnius, D., 1986. Rb–Sr-Isotopengeochemie hydrothermaler Quarze des Bayerischen Pfahles und eines Fluβspat-Schwerspat-Ganges von Nabburg-Wölsendorf/ Bundesrepublik Deutschland. Chemical Geology 58, 259–272.

Jaffey, A.H., Flynn, K.F., Glendenin, L.E., Bentley, W.C., Essley, A.M., 1971. Precision measurements of half-lifes and specific activities of 235U and 238U. Physical Review Series C 4, 1889–1906.

Janoušek, V., Gerdes, A., 2003. Timing the magmatic activity within the Central Bohemian Pluton, Czech Republic: conventional U–Pb ages for the Sávaza and Tábor intrusions and their geotectonic significance. Journal of the Czech Geological Society 48 (1–2), 70.

Johannes, W., Holtz, F., 1996. Petrogenesis and experimental petrology of granitic rocks. Minerals and Rocks, vol. 22. Springer, Berlin. 348 pp.

Kalt, A., Berger, A., Blümel, P., 1999. Metamorphic evolution of Cordierite bearing migmatites from the Bayerische Wald (Variscan belt, Germany). Journal of Petrology 40, 601–627.

Kalt, A., Corfu, F., Wijbrans, J.R., 2000. Time calibration of a *P–T* path from a Variscan high-temperature low-pressure metamorphic complex (Bayerische Wald, Germany), and the detection of inherited monazite. Contributions to Mineralogy and Petrology 138 (2), 143–163.

Kempe, U., Gruner, T., Nasdala, L., Wolf, D., 2000. Relavance of cathodoluminescence (CL) for interpretation of U–Pb zircon ages, with an example of a comparative microprobe study on zircons from the Saxonian Granulite Complex (SCG). In: Pagel, M., Barbin, V., Blane, P., Ohnenstetter, D. (Eds.), Cathodoluminescence in geosciences. Springer.

Keppler, H., 1989. The influence of fluid phase composition on the solidus temperatures in the haplogranite system $NaAlSi_3O_8$–$KAlSi_3O_8$–$SiO_2$–$H_2O$–$CO_2$. Contributions to Mineralogy and Petrology 102, 321–327.

Klečka, M., Matějka, D., 1992. Moldanubian Pluton as an example of the late Variscan crustal magmatism in the Moldanubian zone. 7th Geological Workshop - Styles of superimposed Variscan nappe tectonics, Kutná Hora, abstract. Kutná Hora, pp. 13–14.

Klötzli, U.S., Parrish, R.R., 1996. Zircon U/Pb and Pb/Pb geochronology of the Rastenberg granodiorite, South Bohemian Massif, Austria. Mineralogy and Petrology 58 (3–4), 197–214.

Klötzli, U.S., Koller, F., Scharbert, S., Höck, V., 2001. Cadomian lower-crustal contributions to Variscan granite petrogenesis (South Bohemian Pluton, Austria): constraints from zircon typology and geochronology, whole-Rock, and feldspar Rb–Sr isotope systematics. Journal of Petrology 42 (9), 1621–1642.

Klötzli, U.S., Koller, F., Scharbert, H.G., Höck, V., 2002. Cadomian Lower-crustal contributions to Variscan Petrogenesis (South Bohemian Batholith, Austria): a reply. Journal of Petrology 43, 1783–1786.

Kober, B., 1986. Whole-grain evaporation for $^{207}Pb/^{206}Pb$-age-investigations on single zircons using a double-filament thermo-ion source. Contributions to Mineralogy and Petrology 93, 482–490.

Kober, B., 1987. Single-zircon evaporation combined with $Pb^+$ emitter bedding for $^{207}Pb/^{206}Pb$ age investigations using thermal ion mass spectrometry, and implications for zirconology. Contributions to Mineralogy and Petrology 96, 63–71.

Köhler, H., Hölzl, S., 1996. The age of the Leuchtenberg granite (NE Bavaria, Germany) A revision on account of new U–Pb zircon ages. Neues Jahrbuch für Mineralogie Monatshefte (5), 212–222.

Köhler, H., Müller-Sohnius, D., 1976. Ergänzende Rb–Sr Altersbestimmungen an Mineral- und Gesamtgesteinsproben des Leuchttenberger und des Flössenburger Granits. Neues Jahrbuch für Mineralogie Monatshefte 8, 354–365.

Köhler, H., Müller-Sohnius, D., 1985. Rb–Sr-Altersbestimmungen und Sr-Isotopensystematik an Gesteinen des Regensburger Waldes (Moldanubikum NE-Bayern) Teil 1: Paragneisanatexite. Neues Jahrbuch für Mineralogie, Abhandlungen 151, 1–28.

Köhler, H., Müller-Sohnius, D., 1986. Rb–Sr-altersbestimmungen und Sr-Isotopensystematik an Gesteinen des Regensburger Waldes (Moldanubikum E-Bayern) Teil 2: Intrusivgesteine. Neues Jahrbuch für Mineralogie Monatshefte 155, 219–241.

Köhler, H., Propach, G., Troll, G., 1989. Exkursion zur Geologie, Petrographie und Geochronologie des NE-bayerischen Grundgebirges. European Journal of Mineralogy. Beihefte 1 (2), 1–84.

Konopaśek, J., Schulmann, K., 2005. Contrasting Early Carboniferous field geotherms: Evidence for accretion of a thickened orogenic root and subducted Saxothuringian crust (Central European Variscides). Journal of the Geological Society 162 (3), 463–470.

Kossmat, F., 1927. Gliederung des varistischen Gebirgsbaus. Abhandlungen des Sächsischen Geologischen Landesamtes 1, 1–39.

Kotkova, J., Schaltegger, U., Leichmann, J., 2003. 338–335 old intrusions in the E Bohemian massif — a relic of the orgone-wide durbachitic magmatism in the European variscides. Journal of the Czech Geological Society 48, 1–2.

Kretz, R., 1983. Symbols for rock-forming minerals. American Mineralogist 68 (1–2), 277–279.

Kreuzer, H., Seidel, E., Schussler, U., Okrusch, M., Lenz, K.L., Raschka, H., 1989. K–Ar Geochronology of different Tectonic Units at the northwestern margin of the Bohemian Massif. Tectonophysics 157 (1–3), 149–178.

Krogh, T.E., 1973. Low-contamination method for hydrothermal decomposition of zircon and extraction of U and Pb for isotopic age determinations. Geochimica et Cosmochimica Acta 37 (3), 485–494.

Krogh, T.E., 1982. Improved accuracy of U–Pb zircon ages by the creation of more concordant systems using an air abrasion technique. Geochimica et Cosmochimica Acta 46 (4), 637–649.

Lee, J.K.W., Williams, I.S., Ellis, D.J., 1997. Pb, U and Th diffusion in natural zircon. Nature 390 (6656), 159–162.

Leichmann, J., Koller, F., Svancara, J., Zachovalová, K., 2003. High-K Gabbros related to the durbachites (Jilhava Massif, Moldanubian Zone). Journal of the Czech Geological Society 48 (1–2), 89.

List, F.K., 1969. Ausbildung und Entstehung des Paragranodiorits nördlich und östlich von Deggendorf (südlicher Bayerischer Wald). Geologica Bavarica 60, 95–132.

Ludwig, K.R., 1988. PBdat — a computer program for IBM-PC compatibles for processing raw Pb–U–Th isotope data. US Geological Survey, Open-file Report, pp. 88–542.

Ludwig, K.R., 2003. Isoplot 3.00 — a geochronological toolkit for Microsoft Excel. Berkeley Geochronological Center Special Publication, p. 4.

Massonne, H.J., 1984. Bestimmung von Intrusionstiefen variszischer Granite Mitteleuropas und Neuschottlands anhand der Chemie ihrer Hellglimmer. Fortschritte der Mineralogie. Beiheft 62 (1), 147–149.

Massonne, H.J., Schreyer, W., 1987. Phengite Geobarometry based on the limiting assemblage with K-Feldspar, Phlogopite, and Quartz. Contributions to Mineralogy and Petrology 96 (2), 212–224.

Massonne, H.J., Szpurka, Z., 1997. Thermodynamic properties of white micas on the basis of high-pressure experiments in the systems $K_2O$–MgO–$Al_2O_3$–$SiO_2$–$H_2O$ and $K_2O$–FeO–$Al_2O_3$–$SiO_2$–$H_2O$. Lithos 41 (1–3), 229–250.

Matějka, D., Nosek, T., René, M., 2003. Petrogenesis of two-mica granites of the Ševéntin Massif. Mitteilungen der Österreichischen Mineralogischen Gesellschaft 148, 359–370.

Medaris Jr., L.G., Gent, E.D., Wang, H.F., Fournelle, J.H., Jelinék, E., 2006. The Spačice eclogite: constraints on the *P–T–t* history of the Gföhl granulite terrane, Moldanubian Zone, Bohemian Massif. Mineralogy and Petrology 86, 203–220.

Mezger, K., Krogstad, E.J., 1997. Interpretation of discordant U–Pb ages: an evaluation. Journal of metamorphic Geology 15, 127–140.

Monier, G., Mergoil-Daniel, J., Labernardiere, H., 1984. Générations successives de muscovites et feldspaths otassiques dans les leucogranite du massif de Millevaches (Massif Central français). Bulletin de Minéralogie 107, 55–68.

Nasdala, L., Lengauer, C.L., Hanchar, J.M., Kronz, A., Wirth, R., Blanc, P., Kennedy, A.K., Seydoux-Guillaume, A.-M., 2002. Annealing radiation damage and the recovery of cathodoluminescence. Chemical Geology 191 (1-3), 121–140.

O'Brien, P.J., 2000. The fundamental Variscan problem: high-temperature metamorphism at different depth and high-pressure metamophism at different temperatures. In: Franke, W., Haak, V., Oncken, O., Tanner, D. (Eds.), Orogenic Processes: Quantification and Modelling in the Variscan belt. London, Geological Society of London, vol. 179, pp. 369–386.

Olbrich, M., 1985. Geochemische Untersuchungen der varistischen Magmatite des Vorderen Bayerischen Waldes. Inaugral-Dissertation, München, 161 pp.

Parrish, R.R., 1987. An improved micro-capsule for zircon dissolution in U–Pb geochronology. Chemical Geology 66 (1–2), 99–102.

Pattison, D.R.M., 1992. Stability of $Al_2SiO_3$ triple point: contstraints from the Ballachulish aureole, Scotland. Journal of Geology 100 (4), 423–446.

Petrakakis, K., 1997. Evolution of Moldanubian rocks in Austria: review and synthesis. Journal of Metamorphic Geology 15 (2), 203–222.

Propach, G., Spiegel, W., Schulz-Schmalschäger, M., Wünsch, W., Hecht, L., 1991. Die Genese des Ödwieser Granodiorits. Geologica Bavarica 96, 119–138.

Propach, G., Baumann, A., Schulz-Schmalschäger, M., Grauert, B., 2000. Zircon and monazite U–Pb ages of Variscan granitoid rocks and gneisse in the Moldanubian zone of eastern Bavaria, Germany. Neues Jahrbuch für Geologie und Paläontologie. Monatshefte 6, 345–377.

Propach, G., Bayer, B., Chen, F., Frank, C., Hölzl, S., Hofmann, B., Köhler, H., Siebel, W., Troll, G., in press. Geochemistry and Petrology of late Variscan magmatic dykes of the Bayerischer Wald, Germany. To be published in Geologica Bavarica.

René, M., 1999. Granodiorite Porphyries of the Moldanubian Zone — evidence for the beginnning of the post-Varican extension. Geolines 8, 58.

Richardson, S., Gilbert, M., Bell, P., 1969. Experimental determination of kyanite–andalusite and andalusite–sillimanite equilibrium: the aluminium silicate triple point. American Journal of Science 267, 259–272.

Schaltegger, U., 1997. Magma pulses in the Central Variscan Belt: episodic melt generation and emplacement during lithospheric thinning. Terra Nova 9, 242–245.

Scharbert, S., 1987. Rb–Sr Untersuchungen granitoider Gesteine des Moldanubikums in Österreich. Mitteilungen der Österreichischen Mineralogischen Gesellschaft 132, 21–37.

Scharbert, S., Breiter, K., Frank, W., 1997. The cooling history of the southern Bohemian Massif. Journal of the Czech Geological Society 42 (3), 24.

Scheuvens, D., Zulauf, G., 2000. Exhumation, strain localization, and emplacement of granitoids along the western part of the Central Bohemian shear zone (Bohemian Massif). International Journal of Earth Sciences 89 (3), 617–630.

Schulmann, K., Kröner, A., Hegner, E., Wendt, I., Konopásek, J., Lexa, O., Štipská, P., 2005. Chronological constraints on the pre-orogenic history, burial and exhumation of deep-seated rocks along the eastern margin of the Variscan Orogen, Bohemian Massif, Czech Republic. American Journal of Science 305, 407–448.

Schulz-Schmalschäger, M., Propach, G., Baumann, A., 1984. U/Pb-Untersuchungen an Zirkonen und Monaziten von Gesteinen des Vorderen Bayerischen Waldes. Fortschritte der Mineralogie 62 (1), 223–224.

Scott, D.J., St-Onge, M.R., 1995. Constraints on Pb closure temperature in titanite based on rocks from the Ungava Orogen, Canada; implications for U–Pb geochronology and *P–T–t* path determinations. Geology 23 (12), 1123–1126.

Siebel, W., 1995a. Anticorrelated Rb–Sr and K–Ar age discordances, Leuchtenberg, NE-Bavaria, germany. Contributions to Mineralogy and Petrology 120, 197–211.

Siebel, W., 1995b. Constraints on Variscan granite emplacement in NE-Bavaria, Germany: further clues from a petrogenetic study of the Mitterteich granite. Geologische Rundschau 84, 384–398.

Siebel, W., 1998. Variszischer spät- bis postkollisionaler Plutonismus in Deutschland: Regionale Verbreitung, Stoffbestand und Altersstellung. Zeitschrift für Geologische Wissenschaften 26 (3/4), 329–358.

Siebel, W., Höhndorf, A., Wendt, I., 1995. Origin of late Variscan granitoids from NE Bavaria, Germany, exemplified by REE and Nd isotope systematics. Chemical Geology 125 (3–4), 249–270.

Siebel, W., Trzebski, R., Stettner, G., Hecht, L., Casten, U., Hohndorf, A., Müller, P., 1997. Granitoid magmatism of the NW Bohemian massif revealed: gravity data, composition, age relations and phase concept. Geologische Rundschau 86, S45–S63.

Siebel, W., Breiter, K., Wendt, I., Höhndorf, A., Henjes-Kunst, F., René, M., 1999. Petrogenesis of contrasting granitoid plutons in western Bohemia (Czech Republic). Mineralogy and Petrology 65, 207–235.

Siebel, W., Chen, F., Satir, M., 2003. Late-Variscan magmatism revisited: new implications from Pb-evaporation zircon ages on the

emplacement of redwitzites and granites in NE Bavaria. International Journal of Earth Sciences 92 (1), 36–53.

Siebel, W., Blaha, U., Chen, F., Rohrmüller, J., 2005a. Geochronology and geochemistry of a dyke-host rock association and implications for the formation of the Bavaria Pfahl shear zone, Bohemian massif. International Journal of Earth Sciences 94, 8–23.

Siebel, W., Reitter, E., Wenzel, T., Blaha, U., 2005b. Sr isotope systematics of K-feldspar in plutonic rocks revealed by the Rb–Sr microdrilling technique. Chemical Geology 222, 183–199.

Siebel, W., Thiel, M., Chen, F., 2006. Zircon geochronology and compositional record of late- to post-kinematic granitoids associated with the Bavarian Pfahl zone (Bavarian Forest). Mineralogy and Petrology 86, 45–62.

Simpson, G., Thompson, A., Connolly, J., 2000. Phase relations, singularities and thermobarometry of metamorphic assemblages containing phengite, chlorite, biotite, K-feldspar, quartz and $H_2O$. Contributions to Mineralogy and Petrology 139 (5), 555–569.

Speer, J., 1984. Micas in igneous rocks. In: Bailey, S.W. (Ed.), Micas. Mineralogical Society of America, Reviews in Mineralogy, vol. 13, pp. 299–356.

Stacey, J., Kramers, J., 1975. Approximation of terrestrial lead isotope evolution by a two-stage model. Earth and Planetary Science Letters 26 (2), 207–221.

Steiger, R.H., Jäger, E., 1977. Subcommision on geochronology: convention of use of decay constants in geo-and cosmochronology. Earth and Planetary Science Letters 36, 359–362.

Teipel, U., Eichhorn, R., Loth, G., Rohrmüller, J., Holl, R., Kennedy, A., 2004. U–Pb SHRIMP and Nd isotopic data from the western Bohemian Massif (Bayerischer Wald, Germany): implications for Upper Vendian and Lower Ordovician magmatism. International Journal of Earth Sciences 93 (5), 782–801.

Teufel, S., 1988. Vergleichende U–Pb- und Rb–Sr–Altersbestimmungen an gesteinen des Übergangsbereiches Saxothuringikum/Moldanubikum, NE-Bayern. Göttinger Arbeiten zur Geologie und Paläontologie 35, 1–87.

Troll, G., 1964. Steinbrüche im Intrusivgebiet von Fürstenstein. Geologica Bavarica 52, 1–140.

Troll, G., 1967a. Steinbrüche im Intrusivgebiet von Fürstenstein. Geologica Bavarica 58, 133–144.

Troll, G. (Ed.), 1967b. Führer zu geologisch-petrographischen Exkursionen im Bayerischen Wald. Geologica Bavarica, vol. 58. 188 pp.

Troll, G., Winter, H., 1969. Zur Petrographie und Geochemie von Anatexiten und ihren basischen Einfluessen, im Passauer Wald, Niederbayern. Geologica Bavarica 60, 52–94.

Tropper, P., Deibl, F., Finger, F., Kaindl, R., 2006. *P–T–t* evolution of spinel-cordierite-garnet gneisses from the Sauwald Zone (Southern Bohemian Massif, Upper Austria): is there evidence for two independent late-Variscan low-P/high-T events in the Moldanubian Unit? International Journal of Earth Sciences 95, 1019–1037.

Trzebski, R., Behr, H.J., Conrad, W., 1997. Subsurface distribution and tectonic setting of the late-Variscan granites in the northwestern Bohemian Massif. Geologische Runschau 86, S64–S78 (Suppl.).

Van Breemen, O., Aftalion, M., Bowes, D.R., Dudek, A., Misar, Z., Povondra, P., Vrana, S., 1982. Geochronological studies of the Bohemian Massif, Czechoslovakia, and their significance in the evolution of Central Europe. Transactions of the Royal Society of Edinburgh. Earth Sciences 75, 89–109.

Velde, B., 1965. Phengite Micas — synthesis stability and natural occurence. American Journal of Science 263 (10), 886–913.

Velde, B., 1967. $Si^{4+}$ content of natural phengites. Contributions to Mineralogy and Petrology 14 (3), 250–258.

Vellmer, C., 1992. Stoffbestand und Petrogenese von Granuliten und granitischen Gesteinen der südlichen Böhmischen Masse, Dissertation, University of Göttingen: 112.

Vellmer, C., Wedepohl, K.H., 1994. Geochemical characterization and origin of granitoids from the South Bohemian Batholith in Lower Austria. Contributions of Mineralogy and Petrology 118, 13–32.

Verner, K., Žak, J., Hrouda, F., Holub, F.V., 2006. Magma emplacement during exhumation of the lower- to mid-crustal orogenic root: the Jihlava syenitoid pluton, Muldanubian Unit, Bohemian Massif. Journal of Structural Geology 28, 1553–1567.

Villa, I.M., 1998. Isotopic closure. Terra Nova 10, 42–47.

von Quadt, A., Finger, F., 1991. Geochronologische Untersuchungen im österreichischen Teil des Südböhmischen Batholiths: U–Pb Datierungen an Zirkonen, Monaziten und Xenotimen des Weinsberger Granits. European Journal of Mineralogy. Beihefte 1, 281.

Watson, E.B., Harrison, T.M., 1983. Zircon saturation revisited: temperature and composition effects in a variety of crustal magma types. Earth and Planetary Science Letters 64, 295–304.

Wendt, I., Kreuzer, H., Müller, P., Schmid, H., 1986. Gesamtgesteins- und Mineraldatierungen des Falkenberger Granits. Geologisches Jahrbuch E34, 5–66.

Wendt, I., Höhndorf, A., Kreuzer, H., Müller, P., Stettner, G., 1988. Gesamtgesteins- und Mineraldatierungen der Steinwaldgranite (NE-Bayern). Geologisches Jahrbuch E42, 167–194.

Wendt, I., Carl, C., Kreuzer, H., Müller, P., Stettner, G., 1992. Ergänzende Messungen zum Friedenfelser Granit (Steinwald) und radiometrische Datierung der Ganggranite im Falkenberger Granit. Geologisches Jahrbuch A137, 3–24.

Wendt, I., Ackermann, H., Carl, C., Kreuzer, H., Müller, P., Stettner, G., 1994. Rb/Sr-Gesamtgesteins- und K/Ar Glimmerdatierungen der Granite von Flossenbürg und Bärnau. Geologisches Jahrbuch E51, 3–29.

Whitney, D.L., Teyssier, C., Siddoway, C.S. (Eds.), 2003. Gneiss Domes and Orogeny. GSA Special Paper, vol. 380. Geological Society of America, Denver, CO. 379 pp.

Zulauf, G., 1997. Von der Anchizone bis zur Eklogitfazies: Angekippte Krustenprofile als Folge der cadomischen und variscischen Orogenese im Teplá-Barrandium (Böhmische Masse). Geotektonische Forschungen 89, 1–302.

Zulauf, G., Bues, C., Dörr, W., Vejnar, Z., 2002. 10 km Minimum throw along the West Bohemian shear zone: evidence for dramatic crustal thickening and high topography in the Bohemian Massif (European Variscides). International Journal of Earth Sciences 91 (5), 850–864.